ANL-6343
Reactor Technology
(TID-4500, 16th Ed.)
AEC Research and
Development Report

ARGONNE NATIONAL LABORATORY
9700 South Cass Avenue
Argonne, Illinois

REACTOR DEVELOPMENT PROGRAM PROGRESS REPORT

March 1961

N. Hilberry, Laboratory Director

Division	Director
Chemical Engineering	S. Lawroski
Idaho	M. Novick
Metallurgy	F. G. Foote
Reactor Engineering	B. I. Spinrad
Remote Control	R. C. Goertz

Report coordinated by R. M. Adams

Issued April 15, 1961

Operated by The University of Chicago
under
Contract W-31-109-eng-38

DISCLAIMER

FOREWORD

The Reactor Development Program Progress Report, issued monthly, is intended to be a means of reporting those items of significant technical progress which have occurred in both the specific reactor projects and the general engineering research and development programs. The report is organized in a way which, it is hoped, gives the clearest, most logical over-all view of progress. The budget classification is followed only in broad outline, and no attempt is made to report separately on each sub-activity number. Further, since the intent is to report only items of significant progress, not all activities are reported each month. In order to issue this report as soon as possible after the end of the month editorial work must necessarily be limited. Also, since this is an informal progress report, the results and data presented should be understood to be preliminary and subject to change unless otherwise stated.

The issuance of these reports is not intended to constitute publication in any sense of the word. Final results either will be submitted for publication in regular professional journals or will be published in the form of ANL topical reports.

The last six reports issued in this series are:

September 1960	ANL-6234
October 1960	ANL-6253
November 1960	ANL-6269
December 1960	ANL-6295
January 1961	ANL-6307
February 1961	ANL-6328

TABLE OF CONTENTS

I. WATER COOLED REACTORS (040101)

A. EBWR

1. 100 Mw Modifications - Reboilers

Completion of the modifications to the EBWR plant is still contingent upon the repair of the two primary reboilers. After successfully passing the helium leak test reported in the January Progress Report (ANL-6307), difficulties were encountered in the subsequent head closure weld heat treatment on the No. 1 reboiler. Following the heat treatment one of the tubes developed a fissure and required plugging. In the attempt to plug the tube a leak developed in the weld joint of an adjacent tube. Repairs were finally made and the No. 1 reboiler is expected to be ready for final inspection in early April, 1961.

Repair of the No. 2 reboiler has been completely unsuccessful. Repair attempts resulted in cracks occurring in the heat-affected zone of the weld. Examination of the tubes after removal showed them to be damaged. Severe acid attack of the tubes is evident and the condition of the tubes renders them totally unfit for service. The vendor has agreed to retube the No. 2 reboiler completely and has ordered new tubes and material for a new tube sheet. It is expected that the No. 2 reboiler will be repaired by the latter part of May, 1961.

Considering that the No. 1 reboiler has been exposed to the same conditions of manufacture, repair, and cleaning as the No. 2 reboiler, there is some doubt of its suitability for service. Exploratory tests are being conducted to establish its acceptability.

Investigations were started to determine the causes of the cracking of the Type 304 stainless steel seamless tubing used by the manufacturer. The results of metallographic, corrosion resistance, and simple mechanical tests on virgin tubing materials and on a part of a U-tube removed from the No. 1 reboiler are summarized below:

(1) Metallography - Flow lines of stressed metal were observed indicating either inadequate solution heat treating following tube manufacture, or inadequate resizing operations after solution heat treatment of tubing. No damage to the tube metal structure was evidenced by the one-half hour temper at 900°F which was required for the bent section of the U-tube.

An improvement of the tube metal structure (almost a complete removal of the flow lines) was observed following a 17.5 hour anneal at 900°F. This heat treatment is required of the final head-to-channel steel weld to meet ASME Code requirements. Tube-to-tube sheet welds were exposed to this heat-treating operation.

(2) Corrosion Resistance in Nitric Acid Solutions - The corrosion resistance to 20% nitric acid for two hours at 180°F for three heat treated conditions (as received, 0.5 hour at 900°F, and 17.5 hour at 900°F) was adequate. For the longest heat treat cycle the metal loss was less than 30 mg/sq decimeter (which is about that observed in water).

The corrosion resistance of the three differently heat treated samples in 65% boiling nitric acid (the Huey test: five 48-hour periods) was also adequate. The metal loss was uniform and within the limits of acceptability for corrosion resistance, as defined by this test.

(3) Miscellaneous Mechanical Tests - The tubing was non-magnetic. Tubing was soft (77.78 R_B) in all three of the heat treated conditions.

Four samples of tubing were cut from a non-failed tube removed from the reboiler by the manufacturer. Portions of the tube returned to ANL included the upper part ot the U-tube which has the highest failure history (about 80% of total leaks) as well as the lower part of the same U-tube. Samples of rolled end (expanded into the tube sheet), and of unworked tube about three feet from the rolled end, were selected for examination. The results show the following:

(1) Corrosion Resistance in Nitric Acid - All tube samples, from top and bottom portions of the U-tube, were resistant in 20% nitric acid at 180°F for two hours.

The two samples from the upper part of the U-tube were catastrophically attacked by the boiling 65% nitric acid. After the first 48-hour period (of the five 48-hour periods for the Huey test) the weight loss uncorrected for oxide formation was almost 50%. Further exposure to the 65% boiling nitric acid was therefore discontinued.

Two tube samples from the bottom part of the U-tube sustained weight losses comparable to that of the virgin tubing after the first 48 hour in boiling 65 nitric acid. These samples were returned to the pot for the second exposure.

(2) Miscellaneous Mechanical Tests - Prior to the ANL corrosion tests wall thickness measurements were made on the returned reboiler tube. These indicated that the manufacturer's nitric acid cleaning procedure (2-hour treatment with 20% nitric acid at 180°F) had removed almost 10% of the wall. Walls as thin as 0.032 in. were found and Code specifications required a minimum wall thickness of 0.035 in.

A dye-check examination of the inner walls of the tube sections selected for corrosion resistance tests (tubes were sawed longitudinally by the fabricator) showed only negligibly small flaws. Because of the large differences in corrosion resistance to boiling 65% nitric acid of the two ends of

the same tube, it is suspected that the tubing materials incorporated into the reboilers were incompletely heat treated at the mill. In consequence, the reboiler manufacturer has been requested to supply additional samples of virgin tubing from the center of the tube length as well as of each end, properly identified, for additional investigations.

2. Component Development

a. 17-4 PH Investigation - All nine control rod drives have been removed from EBWR. The 17-4 PH components were inspected using Zyglo Magnaflux, Magnaglow, and ultrasonic tests before and after chrome removal, and found to be free from defects. Considerable difficulty is being experienced in checking the extension racks because of the geometry of the specimen. Experiments are in progress to develop a technique so it will be possible to check cracks in the teeth and at the root of the teeth in the extension racks.

The findings so far reveal that there are numerous surface marks on the material. These are extremely fine and do not allow a discrimination between machine finishing marks and microscopic cracks. Whether the material is cracked or not will therefore be determined by sectioning one of the spare units so as to find out whether the imperfections extend into the body of the material.

The control rod drive test facility has been reworked for the 17-4 PH test program. A space rack, pinion and seal shaft (annealed at 1100°F for 4 hour and air cooled is currently being wear tested. Two additional racks, pinions, and seal shafts are under construction. The design of the rack has been changed to provide teeth on two opposite sides. This change may eliminate the need for straightening after heat treatment.

b. Soluble Poison - The continuous electrodialyzer method now used on a commercial scale for producing demineralized water is being studied for application to boric acid removal from reactor water. A laboratory unit is being constructed for initial studies.

c. Flux Monitoring - The method of transporting flux monitor foils, in the form of small spheres, into the core of the operating EBWR has been improved. A head chain can be mechanically driven through small stainless tubing. The spherical foils are introduced manually or automatically into the tubing and can be accurately located along the length of the tubing by manipulation of the head chain. After a suitable activation time, the chain is again manipulated, carrying the flux monitoring spheres to a collecting device. The spheres are then handled as any other flux monitor foils.

d. Void Simulators - Repairs and modifications were completed on these units. The units were leak tested; three out of the four had minor leaks which have been repaired. Test fitting of these units in enriched thin plate type fuel elements will be done when the reactor pressure head is removed.

e. Instrumented Fuel Assemblies - The instrumented fuel assembly has been completed and the final testing of this element is now being performed in the air-water loop.

f. Control Rod Oscillator - A new and improved oscillator mechanism was designed for EBWR. The original mechanism required experiments to be interrupted while gears were removed and interchanged manually. The new design utilizes electric clutches, and gear changing can be performed remotely. The oscillator will operate at ±12.7 cm below 0.1 cycle/sec down to 0.001 cps, and will be capable of ±2.54 cm at 8 cps with the light hafnium control rod.

The method of controlling the speed of the oscillator hydraulic unit has been modified to provide positive control through the use of limit switches. When the unit reaches a pre-determined top speed in either direction, any further attempt to change the speed will result only in a decrease in speed.

The tachometer-milliammeter speed indicator has been precisely calibrated with a stroboscope. The tachometer is linear throughout the range to be used (100 to 200 rpm), and the milliammeter has been adjusted to provide a maximum ±3% reading error.

3. Examination of Original EBWR Control Rods

The appearance of 2% boron-stainless steel sections (control rods Nos. 2, 4, 6, and 8) as viewed through a three-foot water depth was described on page 3 of the January Progress Report, ANL-6307. All control rod sections have since been examined in a similar manner.

a. Hafnium - The hafnium poison sections (control rods Nos. 1, 3, 5, 7, and 9) are covered with a tightly adherent oxide film, blue-grey in color. No white corrosion products were observed. Spotwelds, employed to assemble the four $\frac{1}{16}$ in. by 5 in. by 5 in. angles into cruciform configuration, appeared sound.

Three cracks were discovered, one each in control rods Nos. 3, 5, and 7. They occur in the 0.5 in. radius, 90-degree angle bend and extend upwards from the hafnium-Zircaloy-2 transition. They are from 11 in. to 14.5 in. long and from $\frac{1}{32}$ in. to $\frac{1}{8}$ in. maximum width.

The cracks are attributed to extreme stress imposed when the original hafnium sheet material was bent into angular form. That material had been embrittled by contamination introduced when iodide crystal bar was rolled into sheet.* It is believed cracks were not initiated, or propagated to any great extent, during EBWR operation. No cracks were observed in control rod No. 9 which had been severely punished by oscillation tests and which had been located at the core center in the region of highest nuclear flux.

b. Zircaloy-2 - There is no indication of distress to the Zircaloy-2 section of any control rod except to the spotwelds at the hafnium transition of No. 9 rod as described on page 3 of the November, 1960, Progress Report, ANL-6269. The sections are covered with a tightly adherent oxide film, grey in color. No white corrosion products were observed.

c. Type 304 Stainless Steel - The Type 304 stainless steel tail sections are covered with a metallic brown tarnish film on their upper ends and a thin white milky film on their lower ends, except the lower ends of control rods Nos. 1 and 3 which are bright and shiny. There is no indication of distress at any portion of these sections.

d. Crud - Crud is deposited on all control rods and increases in density from retrieving tips to the bottom of Zircaloy-2 sections. Crud density is relatively heavy on No. 9 (center) control rod, intermediate on No. 8 (southwest corner), and light on all others.

e. Radioactivity - Boron-steel control rod No. 4 and hafnium control rod No. 9 were cut into 15-cm long (average) pieces as described on page 4 of the October, 1960, Progress Report, ANL-6253. The radioactivity at 1 in. distance from the quadrants of each cruciform piece was measured after the pieces had decayed for eighteen months.

The activity of Zircaloy-2 pieces of both Nos. 4 and 9 control rods are comparable and average 50 r/hr. There is an abrupt increase at the Zircaloy-2 to 2% boron-stainless steel transition of No. 4 rod, from less than 30 to 400 r/hr. The pieces from the top two feet of each rod measure less than 400 mr/hr because of their greater distance from the active core during EBWR operation.

The radioactivity of a given control rod quadrant is an indication of the relative flux that existed opposite the quadrant. The radioactivity measurements show that the flux was uniform around No. 9 control rod at the core center and varied up to 17% around No. 4 control rod in the northeast corner.

---

* "The Experimental Boiling Water Reactor," ANL-5607, p. 33 (May, 1957).

4. Core IA Physics Analysis

A report, EBWR Core IA Physics Analysis, ANL-6305 (see Publication list) has been published. The report is directed primarily toward selection of the optimum loading for Core IA and prediction of its properties. Also included are analyses of some relevant experiments on Core I and, more particularly, on preliminary modifications of Core I towards Core IA.

In order to determine the optimum loading pattern, four different loadings have been considered. Although there are almost an unlimited number of possibilities, the four loadings span, in a general way, the various possibilities.

This study concerns itself primarily with the physics problems of Core IA and gives no information on the possible difficulties at 100 Mw operation due to instability or fuel element failure.

5. Core II

a. Hydrodynamics - Second iteration calculations have been completed for the core and fuel element geometry outlined in the December, 1960 Progress Report, ANL-6295. The circulation characteristics of the core show little change from the satisfactory conditions previously noted. Further hydrodynamic iteration is deemed unnecessary as the incremental changes are well within the accuracy of the correlations now available. Maximum core heat flux estimates decreased slightly from 149.5 to 144.7 w/cm^2 [4.74 to 4.59 x 10^5 $Btu/(hr)(ft^2)$].

b. Schedule - Specifications for Core II are essentially complete and it is expected that requests for bids can be sent out in April.

B. BORAX V

1. Construction

Installation and testing of the piping and insulation is completed, except for minor cleanup work. Some checking, testing, and trouble shooting of the control and instrumentation circuits remains.

The reactor building trench slabs have been repoured and are satisfactory. Painting of the building, pipe and equipment is proceeding. Miscellaneous patching, repairs, etc. to the reactor building and floor slab remain to be done.

ANL has received beneficial occupancy of the demineralized water tank and instrument room in the reactor building and the site for the field chemistry laboratory.

Total estimated completion for the project is 99.5%.

2. Procurement, Fabrication and Installation

The two large core hold-down Belleville springs made of 17-4 PH stainless steel hardened to Rockwell C-34 have been completed and calibrated.

The order for thermocouples for the instrumented boiling fuel assemblies thermocouple "rakes" has been placed with Thermo Electric Company.

Bids on the boiling fuel rod thermocouples are now under evaluation. Two vendors have submitted quotations with several exceptions taken to special treatment requested for fabrication of the tantalum sheaths of the assemblies. A second problem to be resolved on the bids is the method of joining the stainless steel and tantalum-sheathed portions.

Bids have been requested for a two-pen void ratio recorder and associated calculator planned for use with the dual turbine meter arrangement.

Bids have been invited on the reactor vessel extension spool and a depleted-uranium casting for the fuel handling coffin.

All wiring in the control building is completed. Rewiring of the turbine-generator remote control circuits in the turbine building is proceeding. All thermocouples and pressure gages in the turbine building have been calibrated. Installation of relay racks in the reactor building instrument room has started.

Bearings for the turbine-generator are being re-babbitted and remachined. Installation of fiberglass insulation in the turbine building is complete and installation of the wainscoting and painting have started. Installation of the air ejector exhaust system and associated gas monitor is complete. Repairs and insulation on the steam line in the turbine building were finished.

Remodeling of an old demineralizer tank for use in the water storage pit and old reactor vessel cleanup system was completed. Fabrication of the water chemistry sampling panel is nearing completion. Fabrication of the storage racks for boiling fuel rods and assemblies is proceeding.

Installation of furniture and fixtures in the water chemistry trailer is complete and the trailer has been moved to the reactor site.

3. Design

Detailed design of the instrumented boiling and superheater fuel assemblies and pressurized terminal boxes was started. The design of the latch mechanism for the boiling fuel assembly exit flowmeter was completed. Detailed design has been completed for the core structure lifting frame, forced convection baffle lifting frame, boiling fuel rod storage rack, reactor pit bridge, water storage pit bridge, and reactor vessel extension spool.

A middle grid for the boiling fuel assemblies, to reduce the amplitude of the vibrations found in the boiling fuel rods under high flow and void conditions, has been designed and a prototype has been fabricated. Reactivity worth of the addition of the grids in the boiling core is estimated to be -0.5%.

The criticality problem associated with storing fuel in the water storage pit and old reactor vessel has been reviewed and storage layouts have been made.

The IBM 704 program to determine superheater axial fuel and coolant temperature has been checked out and is operational. The feasibility of using irradiated fuel rods for flux mapping is being studied to supplement the use of flux wires and miniature in-core ion chambers.

Writing of the Operating Manual is nearing completion. All the drawings for this Manual are finished and are being checked. Preparation of calculated nuclear characteristics for the Operating Manual is well advanced.

The solution of one of five RE-6 problems to determine the relative worth of voids as a function of radial position has been received. In the "Maximum Accident" section of the Hazards Summary Report, it was assumed that all heat generated in the boiling fuel rods remained in the oxide during the excursions. An investigation of the accuracy of this assumption is proceeding.

4. Development and Testing

a. Boiling Fuel - The 1600 boiling fuel rods returned to the supplier were radiographed and found to be satisfactory. A total of 3040 boiling core fuel rods (5% enriched) have now been received at the laboratory. These rods are being inspected and tested for straightness, leaks, and clad thickness. A total of 483 of the 10% enriched rods have been delivered, as well as 30 thermocouple rods.

b. Superheat Fuel - All nondestructive and destructive tests on the 24 depleted uranium evaluation plates received from the supplier have

now been completed. The results indicate that the plates failed to meet specifications in the following ways:

1) Incorrect external plate dimensions and position of the core relative to the side cladding.

2) Less than minimum required core length due to "fish-tailing" and random configurations at core ends.

3) Flatness not within 0.002 in. per 2 in. length.

4) Carbon content of cladding material greater than 0.03 w/o maximum. (Although the average carbon content does not exceed 0.03 w/o, higher values were found.)

5) Inhomogeneous distribution of uranium in the core blends.

6) Face cladding and core thickness measurements distributed around mean values of 0.007 in. and 0.016 in. respectively, resulting in low face cladding measurements and high core thickness measurements.

7) Excessive stringer lengths and large particle groups.

A summary of the findings of destructive testing is given in Table I. From the table it can be seen that none of the plates examined were acceptable. Consequently, the supplier has been instructed to fabricate a new batch of 24 sample plates for evaluation and approval. It is expected that at least some of the new plates will be available for testing before the end of April. The foregoing results, however, are expected to cause a postponement of the superheat schedule by several months.

Brazing development work for the superheater fuel elements is continuing. Metallographic examination of sections from brazed fuel element type assemblies of stainless steel plates indicated that Coast Metals alloy 60 is equally as effective as GE-81 in attaining sound brazed joints. It was also determined that both acryloid B-72 and polystyrene-benzene carrier cements appear to work effectively in applying the alloy for brazing. Complete integrity of brazed joints has not been found in any assembly made to date.

Brazing samples are also being made to test the performance and corrosion resistance of West Coast Gold and Platinum Co.'s (WESGO) gold-nickel alloy, "NIORO." This alloy is proposed for making the high pressure thermocouple seals at the reactor-vessel-head-nozzle terminal box for both the instrumented boiling and superheater fuel assemblies.

Table I. Results of Destructive Evaluation of 24 BORAX-V Superheat Fuel Plates

Plate No.	Strauss Test	Core Homogeneity	Bond Integrity	Core Thickness	Face Cladding Thickness	Side Cladding Width	End Cladding Length	Oxide Stringer Lengths
FCD 1-7		X		X	X	X		
1-8				X	X	X	NR	X
1-9		X		X	X	X		X
1-10		X		X	X	X		X
1-13		X		X	X	X	X	
1-14		X		X	X	X		
FPD 1-5				X	X			
1-7		X		X	X	X	X	X
1-8	X	X		X	X	X		X
1-10		X		X	X	X		
1-12		X		X	X		NR	X
1-14		X		X	X	X		
HCD 1-8		X		X	X	X		X
1-10		X		X	X	X	NR	
1-11		X		X	X		X	
1-12		X		X	X			
1-13		X		X	X	X	X	
1-14				X	X		X	
HPD 1-7		X		X	X	X		X
1-8		X		X	X	X		
1-9		X		X	X	X		
1-11		X		X	X			
1-12		X		X	X	X		
1-13		X		X	X	X	X	

X = Not Acceptable NR No results Obtained

c. Core Instrumentation and Structure - The exit turbine-type flowmeter for the instrumented boiling fuel assembly has been modified for installation of the latch mechanism and tested in the BORAX V air-water test loop. An error in indicated water flow rate is at present attributed to the influence of the latch mechanism on water flow through the meter. The latch was not installed during factory tests and although test loop data show a deviation (5-15% fullscale) from the original factory data, the calibration is reproducible. Data obtained to date on two-phase flow indicate that the exit meter has given 10% or better agreement with gamma-ray attenuator data over the range of void ratios from 15% to 65% and water flow rates from 30 to 500 gpm (approximately 1 to 20 ft/sec).

A prototype middle grid has been installed in a dummy boiling fuel assembly and preparations are being made for the testing of the effect of this grid on the previously measured vibration of the boiling fuel rods.

A wooden mock-up of the core hold-down structure has been fabricated for installation in the fuel-handling test tank. This mock-up will be used to aid in the design of the routing and support for the in-core instrumentation leads.

d. Control Rods - In an investigation of the 17-4 PH steel problem, a control rod extension shaft made of hardened 17-4 PH has been stripped of its chrome plate, reheat-treated to Rockwell C-33, re-plated, and is being installed in a BORAX V control rod drive for wear tests. New 17-4 PH extension shafts, hardened to Rockwell C-33, are being fabricated.

e. Critical Experiments - Performance of the BORAX V critical experiments in ZPR VII is still delayed pending approval of the hazards report for the experiments. The BORAX V boiling fuel rods for this experiment are on hand.

5. Operations

Plans for a training course for BORAX V operating personnel have been prepared and the course is scheduled to begin in April.

II. SODIUM COOLED REACTORS (040103)

A. General Research and Development

1. ZPR-III

Work on Assembly 32 was completed this month. This assembly contained two columns of fuel and 14 columns of stainless steel in each core drawer.

Assemblies 29-31 had shown that the criticality predictions were inadequate for large dilute power reactors. The cross-section for U^{235} could be shown to account for about half the noted discrepancies, but little quantitative information could be obtained from the basic aluminum and steel cross-section data which seemed to account for much of the remaining discrepancy. Therefore, analysis of Assembly 32, a U^{235} and stainless steel construction, should reveal some information on the adequacy of the steel cross-section values used in the multigroup calculations.

In Assembly 32, a Rossi-alpha measurement yielded the value, $\alpha = 5.37 \pm 0.06 \times 10^{4}$ sec^{-1}. Assuming $\beta = 0.0067 \pm 0.0003$, then the neutron lifetime, $\ell = 12.5 \pm 0.5 \times 10^{-8}$ sec.

The distributed worths of various materials in the core were measured and are listed below:

Material	Distributed Worth (Ih/kg)
Stainless Steel	6.82
Sodium	42.8
Aluminum	26.5

Bunching experiments showed a greater reactivity gain from bunching of the fuel in this assembly than in previous assemblies of this size with different diluents.

Work was started on Assembly 33 which is a modification of the previous assembly. Four $\frac{1}{8}$-in. columns of stainless steel in each core drawer were replaced by two $\frac{1}{4}$-in. sodium-filled stainless steel cans. The critical mass of this assembly was found to be 238 kg of U^{235} as compared to 227.5 kg for Assembly 32.

The volume per cent composition of Assembly 33 is as follows:

Material	Volume Per cent
U^{235}	9.28
U^{238}	0.66
Stainless Steel	63.56
Na	15.81

Reactivity measurements have been made for common reactor materials at the center of the core and for a few selected materials near the edge of the core. The results are shown in Table II.

Table II. Reactivity Worths in Assembly 33

	Reactivity Worths (Ih/kg)			Reactivity Worths (Ih/kg)	
Material	Center	Edge	Material	Center	Edge
U^{233}	366.9	-	Th	-14.1	-
U^{235}	196.7	-	Al_2O_3	92.1	-
Plutonium	349.1	-	$B_4^{10}C$	-1960.0	-
Depleted U	-0.75	2.44	Ph I	-0.13	-
Al	23.5	32.0	Ph II	0	-
St. Steel	1.08	7.6	Pb	1.49	5.36
Na	40.5	60.4	Ta	-30.5	-
C	142.6	118.0	S	-1.8	-
Fe	-0.24	5.1	Nb	-11.6	-
Ni	1.35	9.04	Mo	-6.0	-
Cr	4.35	11.5			

2. ZPR-VI and ZPR-IX

a. Building 315 Construction - Over-all construction of Building 315 is complete inside with the exception of some painting and tile work on the first floor plus service connections to the hoods in the hot laboratory. Outside construction of roads and sidewalks has been delayed by weather conditions.

After installation of the 26-ton exterior door for Cell No. 4, the top hinge broke while the door was partially open. The construction contractor will replace the hinge and effect better alignment on all hinges for this door and the similar one on Cell No. 5.

b. Leak Testing of Concrete Cells - The No. 5 concrete cell is to be pressurized for testing in a manner similar to that used in leak testing a reactor containment shell. Experimental mechanics aspects of this project involve monitoring the strain imposed upon the cell walls during pressurization. Prior to field testing, several laboratory investigations were required.

A stress-coat investigation was made of a typical reinforcing rod used in the construction of the Building 315 facility. The purpose of this study was to determine the direction and relative magnitude of the principal stress across the area between ribs. The significance of this test indicates that removal of reinforcing rod ribs will not be necessary, and a small gage placed between the ribs should be sufficient.

A field installation technique for the strain gages has been developed which is dependable and easy to follow. It is important that the gages be dependable because the entire experimental stress analysis is based upon the response of these detectors.

Installation of instrumentation was completed for the preliminary investigation to establish relationships between surface temperature changes and deflections of the inner surfaces of the faces of the cells.

To determine the effect of transient weather conditions on the cell volume or temperature, 26 thermocouples are being used to monitor hourly the inside and outside temperature distribution on the west wall. At the same intervals, wall deflection measurements are taken as an indication of the magnitude of cell volume changes. Before final testing of Cell No. 5, the seals on the personnel air-lock doors must be repaired. Preliminary checks showed a high leak rate from the space between these doors.

The surfaces of the exposed reinforcement to be instrumented were sand blasted in preparation for the application of the SR-4 strain gages. A tall manometer has been built to record difference in pressures between the cells and the outside. Special protective devices, such as pans which will permit air circulation but will prevent rain and snow from reaching the outside strain gages, were made.

c. Procurement of Components - The bed and table assemblies for the ZPR-VI and ZPR-IX machines have been inspected at the supplier's plant and both units were found to conform with the specified dimensions. One of the two units was operated with a load of 70 tons on each half and performed in a very satisfactory manner. Both assemblies have been accepted, and the first is scheduled for delivery at the end of March with the other following early in April.

Discussions have been held with the suppliers of the instrumentation and consoles regarding the proposed console layout and the interlock circuitry. There seems to be no serious problems in regard to these items, and the supplier believes that he will meet the mid-October deadline for the completion of the installation of the ZPR-VI control console and instrumentation. The final design drawings for the dual-purpose control-safety rod drive mechanisms have been checked and bids requested from potential vendors for the fabrication of the drive mechanisms.

A finished safety rod of the blade type has been tested satisfactorily. A design change was necessary to provide better dimensional control during the boron filling operation and the electro-film baking. It is hoped that venting will eliminate the bulging of the blade sides due to an internal pressure built up at the baking temperatures. This design modification has been completed and another test rod will be made.

The first shipment of the stainless steel matrix tubes for ZPR-VI has been made. Two of the four matrix holding knees have been remachined in order to eliminate warpage produced by the casting operation. Approximately 1200 kg of depleted uranium has been given a protective coating and the coating machine operates in a satisfactory manner.

d. Experimental Program - In the preceding Progress Report (ANL-6328), mention was made of experimental work with a methane-filled proportional counter which might be inserted in a fast critical assembly for spectrum measurements. As a result of the measurements reported last month, the central wire of the counter was replaced by one having a more nearly circular cross section and the resolution for 600 kev protons has been improved to about 8% from the value of 12% observed previously for a gas filling pressure of slightly less than 1 atm.

The previously observed dependence of resolution on gas pressure suggests the need for additional purification of the filling gas. Consequently, a small purification system which will make possible the achievement of better control on the gas purity is now under construction. The inlet and outlet will be flanged to fit a vacuum and filling system. All joints in the system will be heliarc welded and flanged to permit easy cleaning, and stainless steel will be used throughout the system.

Provision is also being made to insert standard alpha sources into the proportional counter for calibration. This will permit a much more thorough study of the effect of gas pressure, impurities, and circuit parameters on the performance. A fast spectrum simulator made of a stack of natural uranium and placed near the leakage face of the ATSR is being considered for further testing of this counter.

Miniature fission chambers containing U^{233}, U^{235}, and U^{238} have been prepared for eventual use in the ZPR-VI facility for measuring the neutron spectrum. Additional chambers containing plutonium and neptunium will be prepared. Tests of these chambers with a 20 ft long coaxial cable have shown a fission-to-alpha signal ratio of approximately 10. Adding a Philco 2N393 transistor as a cathode follower reduced this ratio to about 3. With a good preamplifier, a signal from one of these miniature fission counters can be transmitted through about 40 ft of cable without a cathode follower.

e. Hazards Evaluation - The Doppler effect represents a potential danger for a zero power assembly because the uranium fuel is separated into highly enriched plates and depleted uranium plates. If a sharp nuclear burst should occur in such an assembly the enriched plate will heat faster than the depleted plates by approximately the ratio of the atomic fission probabilities. Thus it may be possible for the positive Doppler reactivity contribution of the U^{235} to outweigh the negative contribution of the U^{238}.

This effect has been examined for ZPR-VI using the recent isotopic energy-dependent parameters determined by Nicholson in APDA-139.* The results indicate that large dilute metal-fueled zero power systems are not dangerous largely because the Doppler contribution of each isotope depends upon the square of the isotopic density, ρ. Since $\rho^2(238)/\rho^2(235)$ can be approximately 50 for a large system, this tends to match, if not outweigh, the reduced Doppler coefficient for U^{238} caused by the low value of $\sigma_f(238)/\sigma_f(235)$. For large oxide-fueled systems, however, $\rho^2(238)/\rho^2(235)$ may be approximately 10 and a serious net positive Doppler coefficient, approaching the shutdown coefficient due to metal expansion, is found for a zero power assembly.

When smaller systems approach the size of EBR-II mockups the parameters given by Nicholson indicate that the positive U^{235} coefficient becomes relatively large. In such systems the $\sigma_f(238)/\sigma_f(235)$ ratio also becomes smaller thus reducing the negative U^{238} Doppler coefficient to the point where the total Doppler coefficient becomes positive but negligible compared to the negative coefficient due to metal expansion on heating.

It should be emphasized that there is necessarily a considerable uncertainty in the theoretical parameters used because of a lack of experimental information on nuclear resonances, which is difficult to obtain. Therefore, there is a need for careful Doppler measurements to be made on these assemblies.

---

*Richard B. Nicholson, "The Doppler Effect in Fast Neutron Reactors," APDA-139, June, 1960.

3. JUGGERNAUT

a. Construction - The JUGGERNAUT is a water-cooled and graphite moderated reactor of the ARGONAUT type. It is to operate at power levels up to 250 kw and provide a versatile facility for nuclear research and component development.

All seven control rods are now in the reactor and have been tested. One rod was cycled for 4,000 times, revealing a faulty drive motor. The motor was returned to the manufacturer and replaced with a spare. The clutch for the rod mechanism did not have enough clearance between the armature and stator and thus caused a slight overloading of the motor. This condition existed on all the rods and was corrected by reducing the diameter of the armature. The remaining rods were cycled 500 times and all appear to be trouble free. The free fall times were recorded to be less than 0.45 sec.

The nuclear chambers have been placed and are operable.

The antimony gamma source was irradiated in the CP-5 reactor for 40 Mw-days in a thermal flux greater than 1×10^{13} n/(cm^2)(sec). The gamma source was installed in its beryllium housing in the reactor and yielded 3.6×10^8 n/sec. With this source, and the chamber in a position expected for reactor operation, the scaler gave a count of 250 counts/sec with the water up and 2,500 counts/sec with the water down; the scale factor is about 5 n/(cm^2)(sec) per count.

The water in the reactor to date has a conductivity of 2 megohms and a pH of 6.6. Samples of the water will be taken daily to determine the efficiency of the cleanup system.

The Hazards Summary Report has been approved and will be submitted to the Commission in early April. A preliminary draft of an Operating Manual has been written. The reactor design report has been started.

b. Critical Experiments - The procedures for the following critical experiments on the JUGGERNAUT have been completely formulated:

1. Approach to Critical
    a. Location and Testing of Neutron Detectors
    b. Fuel Loading
2. Control System Calibration

3. Reactivity Measurement Methods

   a. Period Method
   b. Rod-Drop Method
   c. Subcritical Multiplication

4. Measurement of the Effective Delayed Neutron Fraction (β_{eff})

The procedures for the following experiments are in the planning stage:

5. Power Calibration and Flux Mapping

6. Reactivity Effects

   a. Poison Worth
   b. Fuel Worth
   c. Void Coefficient
   d. Temperature Coefficient

B. EBR-I

1. Operation

The reactor was operated intermittently during the latter part of the month for the purpose of making measurements to determine the total worth of the outer blanket lead cup. Three methods were employed: two of the techniques involved slightly different ways of taking measurements when the cup was dropped, and the third utilized subcritical multiplication. Because of the relatively slow cup drop time (of the order of 300 milliseconds) the analysis is difficult and corrections must be applied to account for the change in reactivity and power level during the drop.

For all three determinations, a pair of small $\frac{5}{16}$ in. diameter fission counters have been used, one at the center of the core and one at a radius of $1\frac{5}{8}$ in. In one case the fission pulses were fed into a count-rate meter and this output in turn was fed to a Brush pen recorder. Several drops were also made recording the scaler pulses directly onto the Brush recorder and switching decades manually.

The second drop method was designed to suppress the relative importance of the drop time by comparing the count rate before the drop to the total count rate obtained after the drop.

The subcritical method is simplest in theory, but is hampered by the poor statistics accompanying the low count rate of subcritical conditions. Analysis of data taken by these three techniques is under way.

2. Mark IV Core

a. Development - The EBR-I Core IV will be loaded with Pu-1.25 w/o Al alloy. The fuel is in the form of 0.235 in. diameter by $2\frac{1}{8}$ in. long cylindrical slugs each of which weighs approximately 25 grams. Each slug has four full length ribs (0.030 in. wide by 0.006 in. high) which are formed by coining the injection cast slugs in a split die. These ribs serve to center the slug in the jacket tube. Four of the fuel slugs are loaded into each fuel rod together with a 3.552 in. long lower and a 7.745 in. long upper beta treated depleted uranium blanket slug. The jacket consists of a 0.300 in. outside diameter by 0.020 in. wall thickness Zircaloy-2 fuel tube. Three equally spaced 48-mil Zircaloy-3 wires are welded longitudinally to this tube to form spacer ribs. The lower end is closed by a locating fitting which is heliarc welded to the tube A tubular spacer and Inconel-X spring are loaded into the tube above the upper blanket. A connnector fitting, threaded to accept a stainless steel extension rod. is fusion welded to the tube after assembly. This fitting is drilled so that NaK may be metered into the assembled fuel rod by means of a hypodermic needle. After NaK filling and level adjustment a plug is inserted into the filling hole and fusion welded to the connector by means of a stored energy arc welder.

Thermocouple rods are modified fuel rods with a 0.080 in. diameter Zircaloy thermocouple protection tube extending axially from the top of the rod to the center of the lower middle fuel slug. Blanket rods and blanket thermocouple rods are similar to the fuel rods except that two depleted uranium slugs replace the four plutonium alloy fuel slugs.

Table III shows the number of fuel elements required and type of slugs for each of the fuel rods.

Table III. EBR-I Core IV Fuel Rods

Rod Type	No. Rods Required	Fuel Slugs per Rod	Depleted U Slugs per Rod
Blanket	120	-	4 solid
Blanket Thermocouple	5	-	3 drilled 1 solid
Fuel	420	4 solid	2 solid
Fuel		3 drilled	1 drilled
Thermocouple	10	1 solid	1 solid

The dual frequency electromagnetic test equipment was used to evaluate the quality of a 12-tube sample of the Zircaloy-2 tubing intended for the Mark IV. These tubes were taken from 1122 feet of tubing recently received from Wolverine Tube. Transverse sections were obtained at about 30 different locations on the tubes to evaluate the defects discovered by the test equipment. Three general types of defects were discovered:

1) Sharp increases of up to 10% in wall thickness over 5° to 10° of the inner circumference and extending sometimes up to several inches along the length of the tube. These cannot be distinguished from radial cracks on the recording produced by the test equipment, but seem to occur infrequently.

2) Radial cracks previously observed in Zircaloy tubing. Since one of the objects of this evaluation was to check the sensitivity of the improved test equipment to small radial cracks, sections were taken at locations believed to contain cracks 0.003 in. deep or less. Cracks of this size occurred in at least half the tubes.

3) A type of defect which resembles a very narrow crack on the order of 0.0001 in. across. These were usually found parallel to the circumference of the tube, but on one occasion one of these defects was found that traversed about 90% of the wall and connected to the outside surface. No decision has been reached on how serious this type of defect is, but previous defect standards do not apply in this case. Another larger sample of this tubing is being evaluated.

In the process of obtaining physical properties of the fuel alloy, thermal expansion curves have been obtained for seven alloy compositions in the "as-cast" condition. At least two dilation runs were made on each alloy specimen. For alloy compositions above 4 a/o Al good agreement was obtained between the expansion curves obtained for the first and second dilation runs. On the other hand, the first expansion curves obtained for two compositions below 4 a/o Al exhibited many inflections which were not evident in the second dilation. In each of these latter compositions satisfactory agreement was observed between the expansion curves of the second and third dilations. Furthermore, the expansion curves obtained in the second and third dilations for these lower compositions exhibited an abrupt drop at 400°C. These alloy specimens will be homogenized at 425-450°C for 100 hours and their expansion coefficients will be determined again. It is hoped that the expansion data obtained on the homogenized alloys will help to explain the data obtained thus far on the "as-cast" material.

b. Fabrication - Production of fuel elements is in progress with 587 slugs produced as of March 17. The method developed consists of precision injection casting nine fuel pins (18 in. x 0.234 in.) at a time in Y_2O_3

coated, high-silica glass molds. A rod-parter is used to cut slugs from the cast rods. These are then upset in a coining die to form the four ribs. The slugs are machined to final length and the edges chamfered.

A total of 2912 feet of 0.257 in. I.D. Zircaloy-2 tubing stock for Core IV jackets has been received. Of 2028 feet of this tubing inspected, 63% has been accepted for fuel and blanket rod jackets.

Over 16% of the finish-machined rod tips are available for assembly.

Enough Zircaloy-2 wire for 32% of the required jacket spacer ribs has been fabricated by the Laboratory and eddy-current inspected.

All of the filler plugs, 83% of the NaK level spacers, and 18% of the fuel connectors are finish-machined and ready for assembly.

Machining of the depleted uranium blanket slugs from available rod stock has been started.

Assembly and welding operations have been less thoroughly rehearsed than other operations because of the critical shortage of satisfactory Zircaloy tubing. The problem is to load the tubes, weld, fill with sodium and bond without exposing the exterior of the jacket or the weld to contamination. The internal parts are inserted while the jackets are attached to multiple fittings on a vinyl pouch. The loading arrangement is shown in Figure 1 and, for obvious reasons, the pouch has been named "the cow."

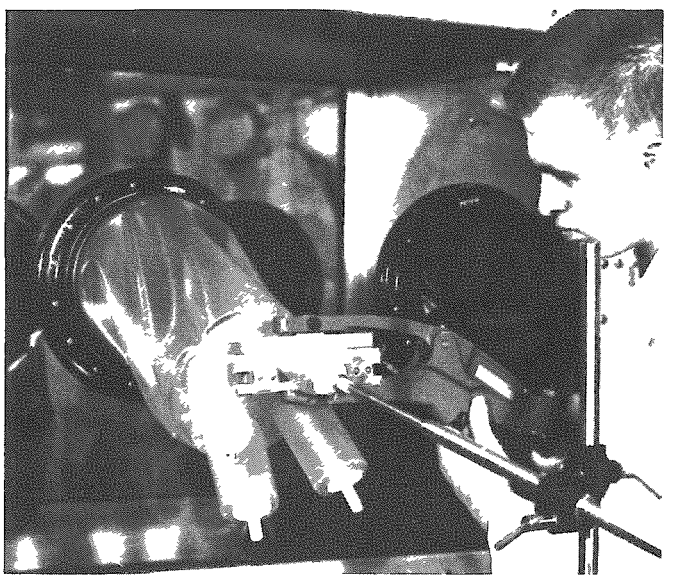

Figure 1

Dielectrically Sealing a Loaded Fuel Specimen from a High Level Contaminated Hood Line using a Multitubulated Vinyl Pouch.

The edges of the fuel tubes are protected by a thin polyethylene funnel through which the internal parts including the fuel slugs are loaded. A sectional view of this fitting is shown in Figure 2. After loading, the vinyl tubulation above the fuel element is dielectrically sealed and the assembly transferred to a sodium filling and welding line where the connector is inserted and the heliarc girth weld is made. NaK filling is done in the vertical position with the rod in a vacuum pressure chamber. A hypodermic filling tube is inserted into the rod, the chamber is evacuated and a measured quantity of sodium is injected while the rod is gently vibrated. The chamber may be pressurized after filling to force the NaK into the bond annulus. After filling, the plug is inserted and fusion welded to the connector by an arc discharged from a capacitor bank.

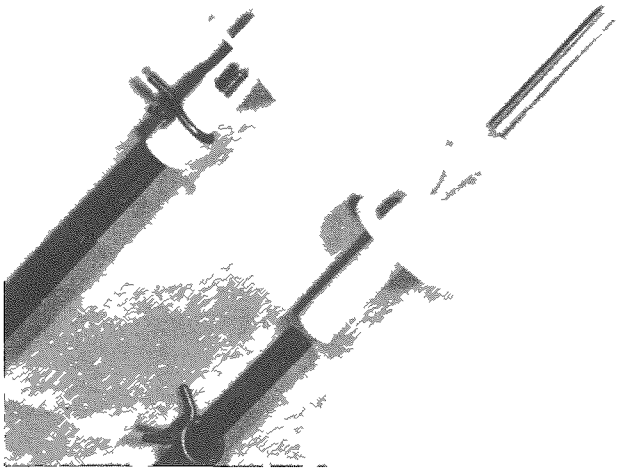

Figure 2

Exploded and Sectioned Views of Vinyl Loading Fitting. Spring Hose Clamp and Polyethylene Funnel used to Prevent Contamination of EBR-I Fuel Tube.

Leak detection will be by both the pressure and mass spectrometer techniques described in previous reports, and the bond and NaK levels will be established by methods similar to those previously used. Each fuel element will be X-rayed to indicate that all components are properly positioned and that the desired sodium level has been achieved.

C. EBR-II

1. Construction

The following tabulation presents the approximate status of the construction contracts as of March 14, 1961:

Building	% Completion
Power Plant (Package 2)	100
Reactor Plant (Package 2)	100
Sodium Boiler Plant (Package 3)	89
Fuel Cycle Facility (Package 3)	82

a. Sodium-Boiler Plant - The Progress Report for February (ANL-6238) noted the Laboratory's concern that orderly prosecution of the EBR-II Experimental Program could hinge upon early procurement and installation of the flexible seals (a contractor-procured item). This item, and all other Package 3 work in the Reactor Plant, has been removed from the Package 3 contract by change order and will be performed under Package 4.

The rate of construction progress is very slow. During the past eight weeks the percentage completion has averaged about 1% per week. Unless the present pace increases, the Contractor will not finish this portion of Package 3 by June 1 (the present estimated completion date). Any significant slippage of this schedule could have a serious effect upon the startup schedule of the facility.

2 Installation of Equipment - Package 4

Installation work within the reactor plant falls into two general categories: (a) mechanical, comprising approximately 70% of the total; and (b) electrical, approximately 30%. For convenience in scheduling and supervising the work in the field, the mechanical work is divided into 43 major jobs, or packets, and the electrical into 5 packets. Work on 42 of the mechanical packets and all 5 of the electrical packets has been started. To date, approximately 93% of the total mechanical work and 77% of the electrical work has been completed.

a. Gripper and Hold-down Mechanism - The function of the gripper and hold-down mechanism is to insert and extract subassemblies from the reactor vessel. This mechanism performs its operations remotely. It incorporates several design features which lend added reliability to the fuel transfer process, such as sensing devices, force-limiting devices, and holddown of adjacent fuel subassemblies to prevent their simultaneous removal. The mechanism is necessarily complex and requires extremely careful alignment and adjustment of many interconnected assemblies. Mechanical installation of this device is essentially complete. Precise adjustment and alignments will be performed during equipment testing and check-out phases prior to the dry critical experimental program.

b. Storage Rack Mechanism - The function of the storage rack mechanism is to provide a means for temporary holdup of new and spent fuel (and blanket) subassemblies. The rack is suspended from the primary tank cover, and is fully submerged in the tank sodium at all times to permit natural convection cooling of spent subassemblies within it. The rack is cylindrical, with a capacity of 75 subassemblies. The associated drive mechanism provides both vertical and rotational movement of the rack to permit either insertion or removal of a subassembly from the rack by the

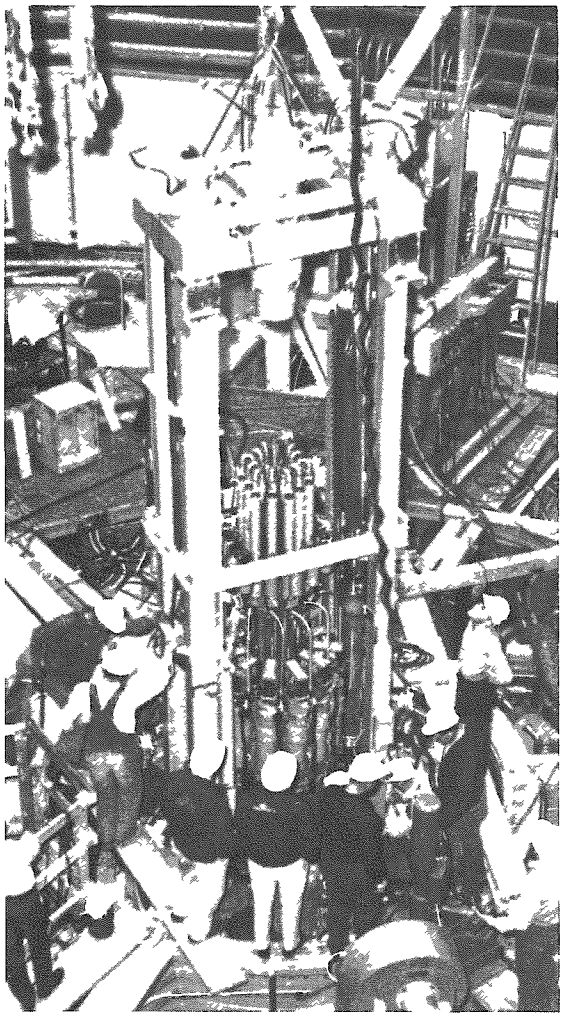

Figure 3

Installation of Upper Structure of Reactor Vessel Cover Lifting Mechanism

transfer arm. Mechanical installation of this device is essentially complete. As with the gripper and hold-down mechanism, precise adjustments and alignments may be required later during certain phases of testing and checkout.

c. Reactor Vessel Cover Lifting Mechanism - In the February Progress Report (ANL-6328) it was noted that this device was installed. Figure 3 shows the upper structure of this mechanism being lowered into place over the cluster of control rod drives.

d. Sodium Purification System - A recirculating cold trap system is used for continuous primary sodium purification. This system permits the concentration of impurities to be maintained at or near their greatly reduced solubility limits for temperatures just above the melting point of sodium. Cold trap precipitation is effective in maintaining low concentrations of such impurities as sodium hydride, many fission products, and particularly sodium monoxide.

The cold trap consists of a 500-gallon tank filled with Type 304 stainless steel wire mesh to provide supplementary surface area to enhance sodium crystallization and deposition. A regenerative heat exchanger is incorporated to reduce over-all heat losses in the cold trap system. The cold trap operational temperature of 350°F is maintained by a NaK coolant loop.

Two types of analytical devices are installed in the primary sodium purification system for the purpose of determining sodium quality: (a) a plugging indicator for dynamic side stream oxide monitor, and (b) a sodium sampler for physical removal of sodium from the main stream. The plugging indicator loops and sampling points are located on both the sodium inlet and outlet side of the cold trap. These devices will be used to check the efficiency of the cold trapping operations and to provide sampling points for chemical and radiological analysis of the sodium before and after the purification cycle.

The plugging indicator is a device used for monitoring oxygen concentrations in flowing systems. It consists of a regenerative heat exchanger, a plugging valve containing both a fluted valve stem for increased surface area when closed and a thermocouple, and a throttling valve for flow control. The plugging indicators are operated across a small pressure difference which is used to regulate flow, and the throttle valve is used for fine adjustment of flow.

During operation sodium is cooled and passed through the closed plugging valve at a constant flow rate. When the saturation temperature of the sodium is reached sodium oxide is precipitated out on the surface area of the orifice causing a reduction in flow. The oxide concentration of the sodium is then determined from the temperature solubility curve of oxygen in sodium.

The plugging indicators used in the EBR-II are of ANL design, and past experience has shown that the instrument is reliable and the results reproducible.

The sampler in the primary sodium purification system is employed to extract sodium from the primary coolant stream for the purpose of making sodium oxide determinations below the limits of detectability of the plugging indicator, and for physical removal of small sodium specimens to permit analyses of gross impurities in the sodium.

For making oxide determinations, the sampler utilizes the vacuum distillation analytical technique developed at the Laboratory. A representative sodium sample is introduced remotely into a sample cup lined with metal foil and the sodium is separated from its nonvolatile impurities by vacuum distillation. After a sufficient distillation time, the sampler is filled with inert gas and the metal foil is withdrawn. The residue on the foil is then analyzed by standard chemical or radiological methods.

The bulk sodium samples consisting of 1 cc of sodium metal will be withdrawn from the primary coolant stream for the purpose of determining the presence of impurities, other than oxide, and the concentration of these impurities by radiochemical, spectrometric, and wet chemical techniques.

Figure 4 is a view of the wall between the sodium sampling cell and the sodium purification cell. The cavity in the lower center of the wall is for the sodium sampler. Directly above and to the left is the penetration and ball bearing mounting for a periscope which will be used by occupants of the sodium sampling cell to observe the inside of the sodium purification cell. Above the cavity and to the right are the six manual operators for sodium plugging indicator valves. At the extreme right can be seen part of the NaK-silicone heat exchanger and the NaK lines running into the sodium purification cell and to the cold trap.

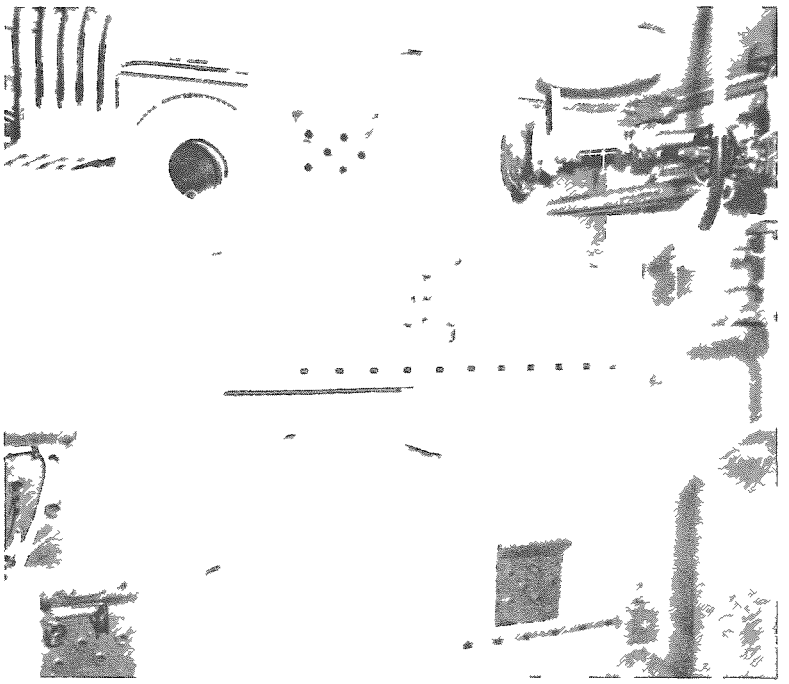

Figure 4

Sodium Sampling Cell

The control valve just below the ceiling and under the lighting fixture is also in the NaK line. A better view of these last-mentioned pieces of equipment can be seen in Figure 5. Also shown in this picture are the AC-EM pump for the NaK (to the right of the heat exchanger) and the retention basin for collection of any possible NaK leakage from above.

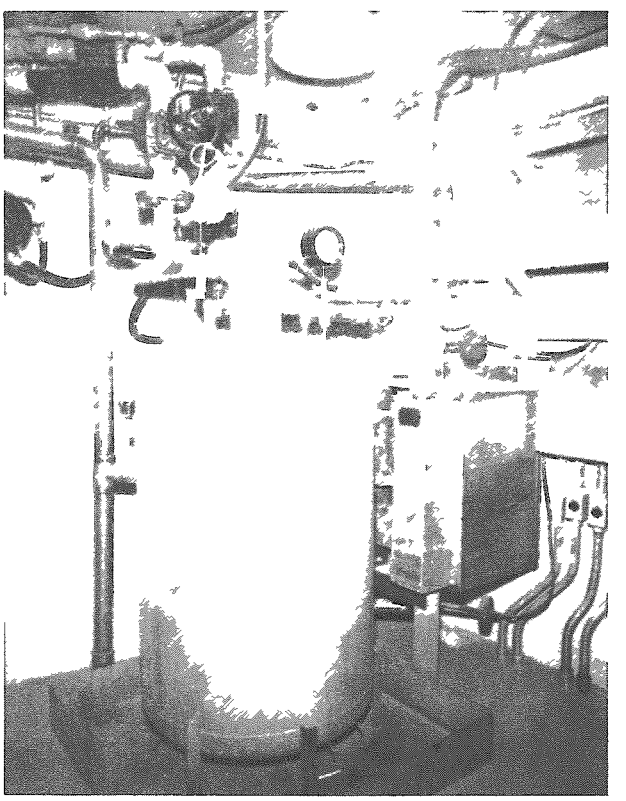

Figure 5

Sodium Sampling Cell Showing AC-EM Pump and NaK Silicone Heat Exchanger

e. Argon Purification System - The sodium in the primary tank is blanketed by argon. Pressure and makeup for this blanket as well as cleanup are provided by the argon purification system. Figure 6 shows the floating head tank installed in the argon purification cell.

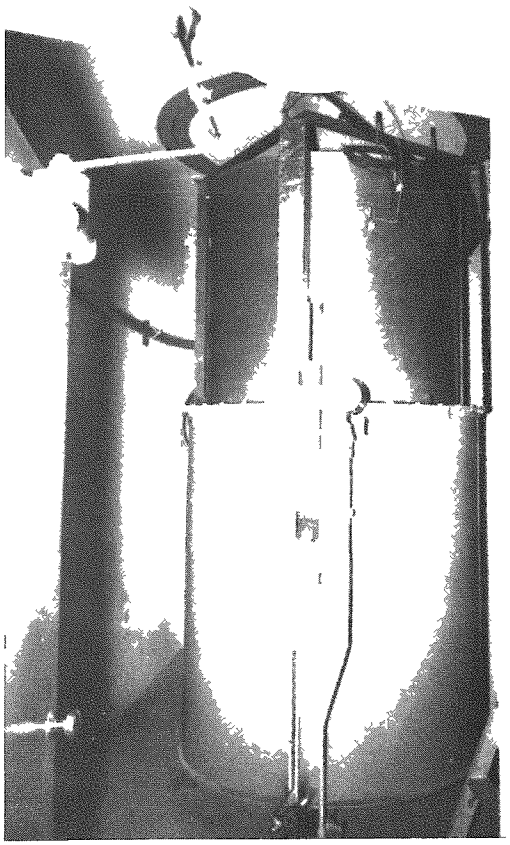

Figure 6

Floating Head Argon Tank

f. Power Plant - The continuous power supply equipment has been rearranged to eliminate overloaded circuits mainly to the Leeds and Northrup control panels. This problem was discovered as a result of a load study on the continuous power supply system. Figure 7 shows the back view of the panels and equipment including the motor-generator sets.

Engineering

Design drawings for modification and correction of the nuclear control circuits have been issued to the field. These include modifications to the shutdown circuit such as the addition of a manual safety rod scram, scram on loss of high voltage to ion chambers in Channels 4, 5, and 6, and an interlock to prevent fuel handling unless all 12 control rods are fully down. The reactor cover switch has also been interlocked into the fuel handling control circuit.

Modifications to the nuclear instrumentation and control circuits for the dry critical experiment are being prepared for issue to the field. A control rod switch simulator design has been issued for fabrication in the field. This simulator is to provide the required electrical connections when a control rod is disconnected or removed from its position for the critical experiments.

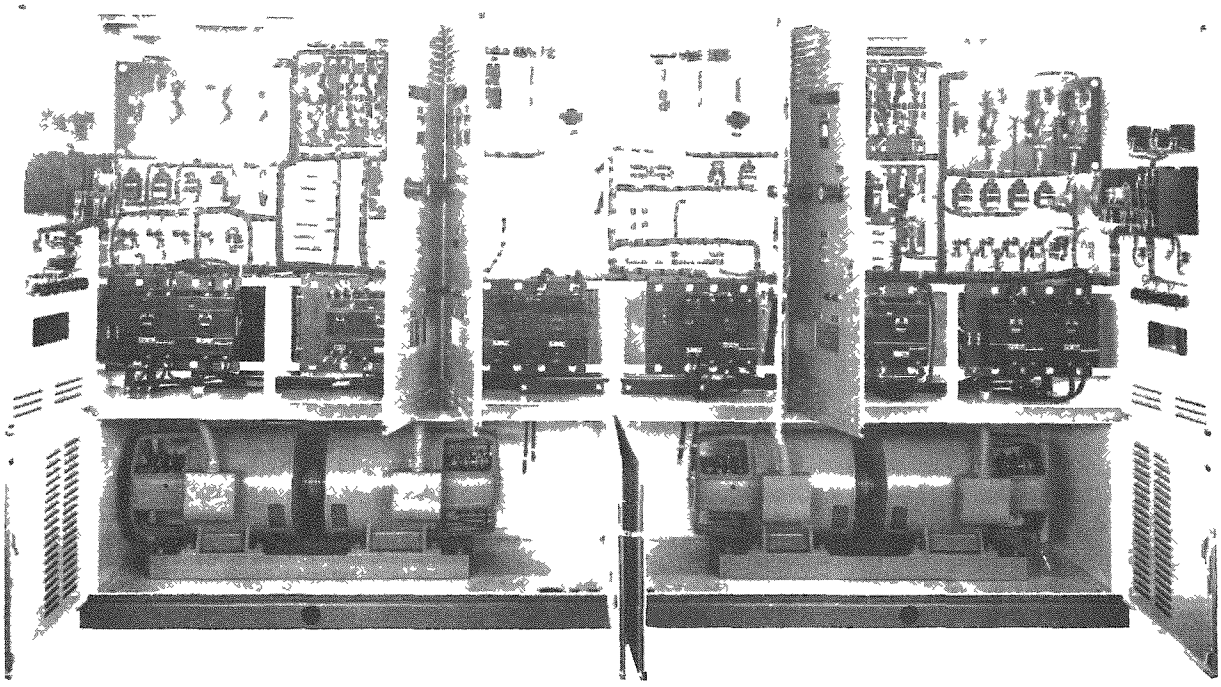

Figure 7

Rear View of Continuous Power Supply Panels

A number of special devices necessary for dry critical experiments are now in design, fabrication, and/or procurement. The list in the February Progress Report (ANL-6328) has been expanded to include the following:

a. Viewing Apparatus

(1) Two periscopes for remote observation of fuel handling within the primary tank during dry critical experiments (and/or during sodium filling).

(2) A number of mirrors to be positioned temporarily within the primary tank for use in conjunction with the periscopes.

(3) Windows to be employed on certain primary tank nozzles to facilitate observations in the primary tank.

(4) A closed circuit television camera to be mounted inside the primary tank with the pan and tilt mechanism for monitoring operations.

(5) Lighting facilities required for the above.

b. Special Assemblies and Thimbles

(1) One in-core thermocouple subassembly with the thermocouples attached to the fuel element tubes to monitor temperature during the dry critical experiments.

(2) Two in-core instrument thimbles to be located in the inner blanket and each containing a high temperature fission counter and an absolute fission counter.

(3) Two neutron source thimbles, one with an inner blanket adapter and one with an outer blanket adapter. Each is a beryllium bearing thimble for the antimony-beryllium neutron source.

(4) Several neutron source rod assemblies of various strengths.

(5) Two source shielding thimbles to provide temporary housing and to shield source rods in blanket positions. These permit intermittent personnel access to the immediate vicinity of the reactor vessel during shutdown periods of the dry critical experimental program.

(6) One fission foil traverse subassembly for the inner and outer blanket, each to accommodate a number of pairs of enriched and depleted cadmium covered uranium foils.

(7) An oscillator rod assembly and thimble based on utilization of certain parts of a standard type control rod drive.

c. Special Equipment for Experiments and Tests

(1) Two rod drive sequence simulators to satisfy operational and safety interlocks and power and control circuits when control rod drives are removed for various dry critical experiments.

(2) A dry critical subassembly loading rig as described and depicted in ANL-6299, "EBR-II Dry Critical Experiments."

(3) Control rod drive testing equipment (and dummy control rod) necessary for complete in-core checkout and performance testing of the rod drives.

(4) Structural deflection system and instruments necessary to investigate the deflection of the primary tank cover and support structure during high temperature operation and sodium loading.

(5) A temporary air circulating system to be used in the primary tank to assure reasonably uniform temperature distribution during isothermal temperature coefficient measurements and other dry critical and post-dry critical experiments.

4. Procurement

The shield plug section of the sodium-to-sodium heat exchanger contains the neutron shielding material, the sodium entrance and exit piping, and an expansion bellows (see Figure 8, Progress Report, ANL-6328). The expansion joint and the entrance and exit piping have been installed and helium leak tested at the vendor's shops. The internal piping of the heat exchanger is now complete up to the shield plug cover plate. The carbon steel shielding material is also in place and the remaining shielding material is being installed. Delivery will be made during April.

Delivery of the fuel handling center from the Datex Corporation is expected about April 7. This improvement in delivery is a result of assistance by the AEC and others in expediting delivery of some of the components. Preparation of the interconnection diagrams for the field installation is progressing satisfactorily and will be completed in adequate time so as not to delay installation.

The final shipment of equipment for the reactor plant from Argonne, Illinois to the site has been made.

5. Reactor Analysis

a. Hydraulic Studies of EBR-II Reactor and Fuel Subassemblies - The effect of inadvertant reactor operation with either a core, inner blanket, or outer blanket subassembly omitted has been investigated. The increase above normal in required pump output flow for the first two cases is more than 4.5%. The case of omission of an outer blanket subassembly would not be observable as a change in pump flow but a 9% increase in the flow to the reactor lower plenum would be apparent. In no case would the normal hold-down force of subassemblies adjacent to the missing subassembly be significantly affected.

The condition of reactor operation without any subassemblies in the reactor was calculated. This operation could be considered for purposes of flushing the primary flow circuit. Since the pump discharge pressure is only about 7.5 psi (above hydrostatic) when 9000 gpm is delivered by the two pumps, the proper operation of the pump's sodium "lubricated" bearing cannot be assured. About half the total flow passes out the bottom of the reactor and sweeps the bottom of the primary tank, which is not desirable. This method of primary system operation is therefore not recommended.

Calculations of the leakage out of the primary sodium system to the bulk sodium were completed. The total leakage from pump discharge to heat exchanger outlet is 470 gpm at 100% power with the 67-core geometry.

Since the individual subassembly hold-down forces vary with changes in reactor configuration, the hold-down (or seating) forces were recalculated for various percentages of flow with the 67-core geometry. None of the forces for the core, inner blanket, or outer blanket subassemblies drop below the 73-lb dead weight of the individual core subassembly in sodium at flows up to 100% of full flow. The hold-down force of the outer blanket subassembly drops to 68 lb at full flow.

b. Stress Analysis - Further investigation is being conducted on the spring-loaded reactor hold-down devices. Analysis includes a study of the stress concentration areas and the over-all performance.

An additional analysis has been made of the danger from missiles formed by an excursion during the Dry Critical Experiments. The containment system was found to be adequate.

c. Shield Analysis - Maximum heating in the EBR-II sodium tank wall nearest the fuel storage basket was calculated. Assuming all basket storage positions in the two outer rows filled with core subassemblies that have cooled one hour after infinite operation, calculations gave a value of 0.23 watts/cm^3 for the maximum heating in the steel of the tank wall due to radiation from the subassemblies. The sodium should dissipate this amount of heating without any harmful stresses being developed.

d. Use of Boron Carbide - A rather extensive literature search was concluded on the subject of boron carbide and its properties. It is proposed to use boron carbide (B_4C) as a poison material in certain of the control rods as a method of increasing the rod worth. In case it is found necessary or desirable to maintain this feature permanently for actual operating conditions, information is needed regarding stability of this compound under operating conditions, and its compatibility with sodium (in case of a leaky container) and various materials which might be used for the container tubes.

It was found that this material is stable chemically at the temperatures involved; however, there is the possibility that when in contact with some materials, such as stainless steel, excess carbon (which is always present to insure complete carburization of the boron) might migrate into the can walls causing embrittlement.

Also, when exposed to neutron bombardment, the B^{10} reacts producing an alpha particle. The alpha particles find electrons to form helium. Theoretically, there is room in the lattice for helium generation equivalent to approximately 8% burnup which would far exceed the proposed lifetime for this poison loading; however, thermal effects and fast neutron damage dislodge a portion of the helium atoms, some of which find their way into voids and the surroundings. This free helium raises the pressure in the tubes. At the temperatures existing in control rod locations, and because of the heat generation by the (n,α) reaction and the high flux environment, a substantial fraction of the helium should be released. Stability with sodium is good although under irradiation the carbide in the form of hot pressed rods tends to disintegrate as the degree of burnup increases. This effect is aggravated to some extent by the presence of sodium in the voids.

For actual operating conditions it appears that containment for the B_4C is essential. Also, since all components in the core must be stainless steel if in contact with sodium, a protective covering, wrapped around or plated on the B_4C is necessary to prevent carburization of the stainless steel container. The container must also be designed to allow for a pressure increase by helium release. Since the fraction of the helium generated which might be released is controversial, it seems advisable to design for 100% release to be safe, although this is obviously conservative.

The selection of tube diameter and wall thickness involves consideration of thermal stresses, bursting stresses, heat generation and dissipation, temperatures, helium generation, allowable pressure, per cent burnup in postulated lifetime, sodium flow, and geometry. In addition, certain other considerations, such as end closure configuration, welding, leak testing, effects on the control rod structure, shielding, etc., must be taken into account. Calculations for burnup were made for several alternative designs.

e. Effects of Foreign Particles on EBR-II Fuel Element Temperatures - Additional studies have been conducted to determine the probable effect on EBR-II core temperatures of foreign particles which might lodge in the core coolant passages. Earlier work on this subject showed that single foreign particles which are retained individually can cause only negligible effects. The current studies considered the more improbable situations which would result if a large number of foreign particles should progressively accumulate to form a flow channel blockage of comparatively substantial size.

Five different cases of the latter type of blockage were investigated and are discussed here. For all cases the following conditions apply:

(1) The reactor is at steady-state, full-power operation (62.5 Mw).

(2) The maximum fuel and fuel-clad interface temperatures presented apply, respectively, to the fuel elements which normally exhibit the highest fuel (about 1197°C) and interface (about 1060°F) temperatures.

(3) The foreign particle accumulations are assumed to have the same thermal conductivity as Type 304 stainless steel.

(4) Under the worst flow transient conditions envisioned (cessation of all pumping power with subsequent reactor scram) maximum fuel and interface temperatures never exceed those given here. Pertinent assumptions for this transient are: total rod reactivity worth = 0.05 and initial rod insertion = 80%.

(5) For evaluation of the results it should be noted that the fuel-clad eutectic melting point is 1340°F.

(6) Except for Case 4, the foreign particle accumulations are considered to extend for the entire axial length of the fuel elements.

The foreign particle accumulation designated as Case 1 is shown in Figure 8. The accumulation increases the maximum fuel temperature from the normal value of about 1197°F to about 1213°F and increases the maximum fuel-clad interface temperature from the normal value of about 1061°F to about 1165°F. The temperature increases are due entirely to increased thermal resistance between the fuel element and the coolant.

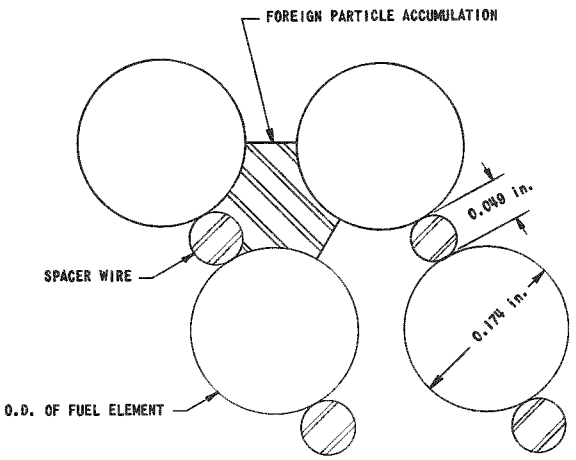

Figure 8

Foreign Particle Accumulation (Case 1)

Figure 9 pictures the Case 2 type of accumulation and its effects on fuel and interface temperatures. The indicated width of the

covered area is measured at the element clad OD. The temperature increases again are due entirely to increased thermal resistance between the fuel element and the coolant.

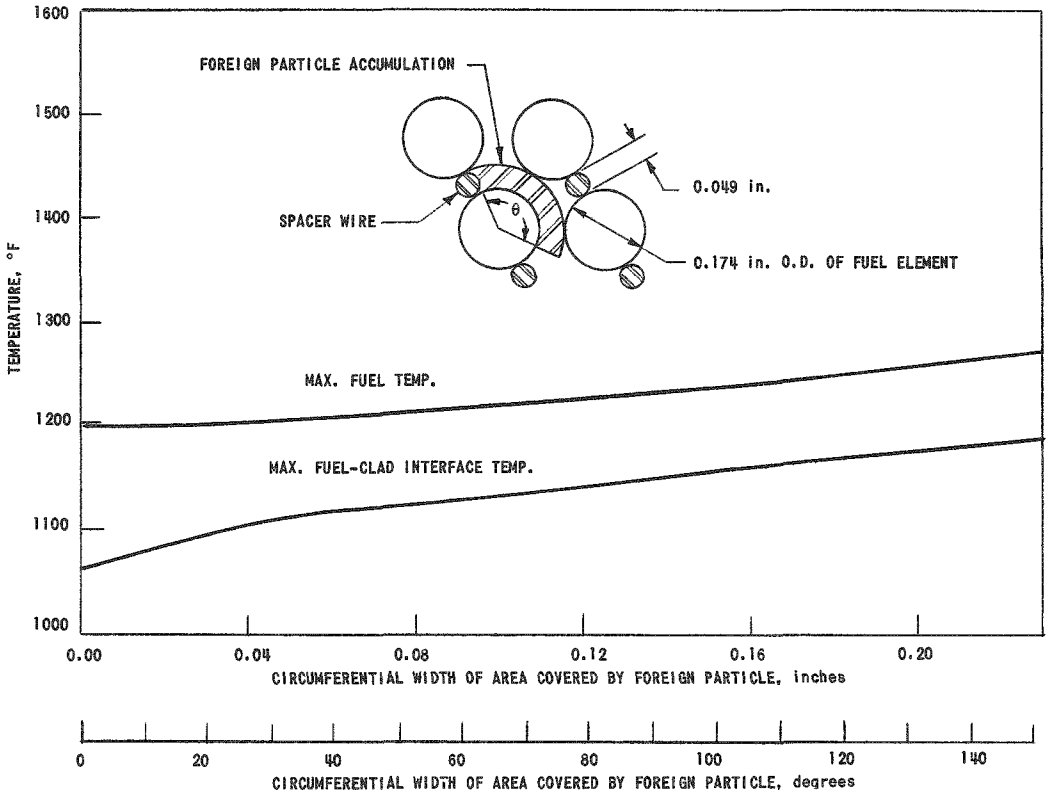

Figure 9

Foreign Particle Accumulations (Case 2) and Their Effects on EBR-II Core Temperatures

The Case 3 type of accumulation is sketched in Figure 10. The accumulation increases the maximum fuel temperature from the normal value of about 1197°F to about 1261°F and increases the maximum fuel-clad interface temperature from the normal value of about 1061°F to about 1173°F. The temperature increases are due entirely to increased thermal resistance between the fuel element and the coolant.

Figure 11 illustrates the effects on fuel and interface temperatures of the Case 4 type of accumulation, which is considered to occur in the region of the fuel element grid bars. The temperature increases then are due entirely to higher coolant temperatures, caused by reduced coolant flow rates.

In Figure 12 the Case 5 type of accumulation and its effects on fuel and interface temperatures are shown. This type is identical to that for Case 1 except that a number of blocked channels are considered to

occur in the same subassembly. However, no fuel element is in contact with more than one blocked channel. The temperature increases are caused both by increased thermal resistance between fuel element and coolant and by higher coolant temperatures resulting from reduced coolant flow rates.

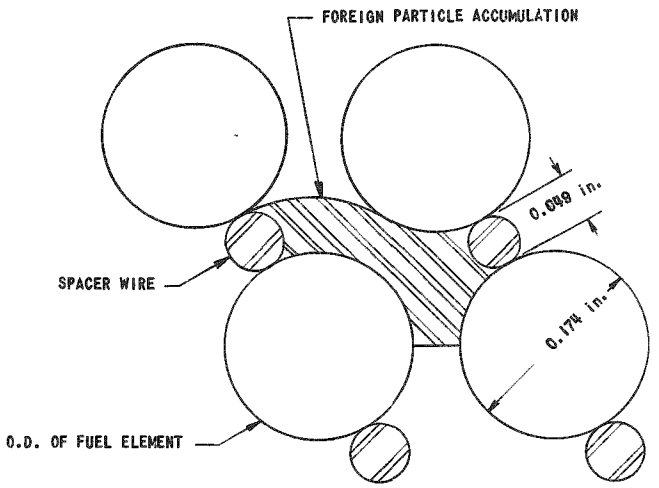

Figure 10

Foreign Particle Accumulation (Case 3)

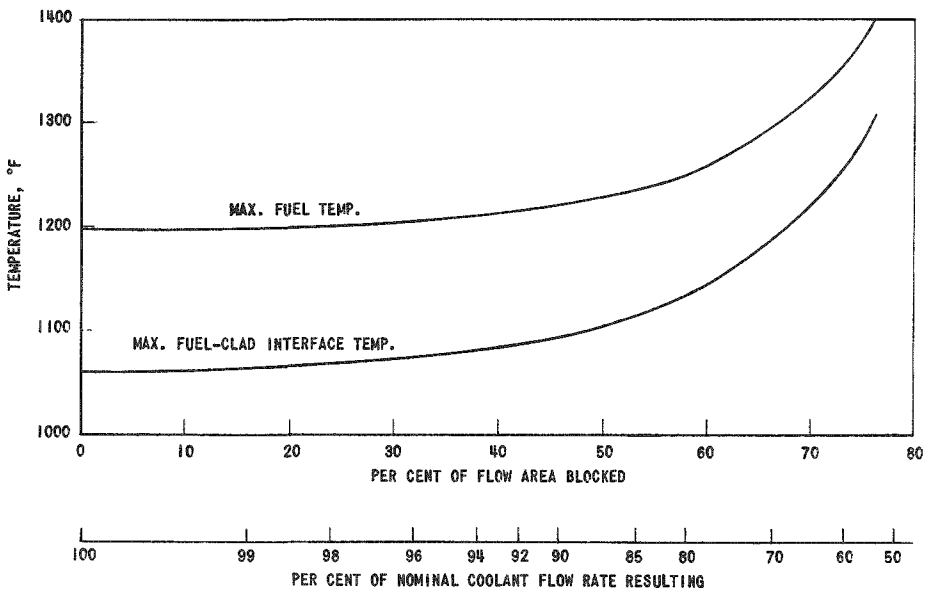

Figure 11

Foreign Particle Accumulations (Case 4) and Their Effects on EBR-II Core Temperature

The results given here are considered conservative and are highly reassuring. It is evident that extensive accumulations of foreign particles can be sustained within the EBR-II core without developing unacceptably high temperatures.

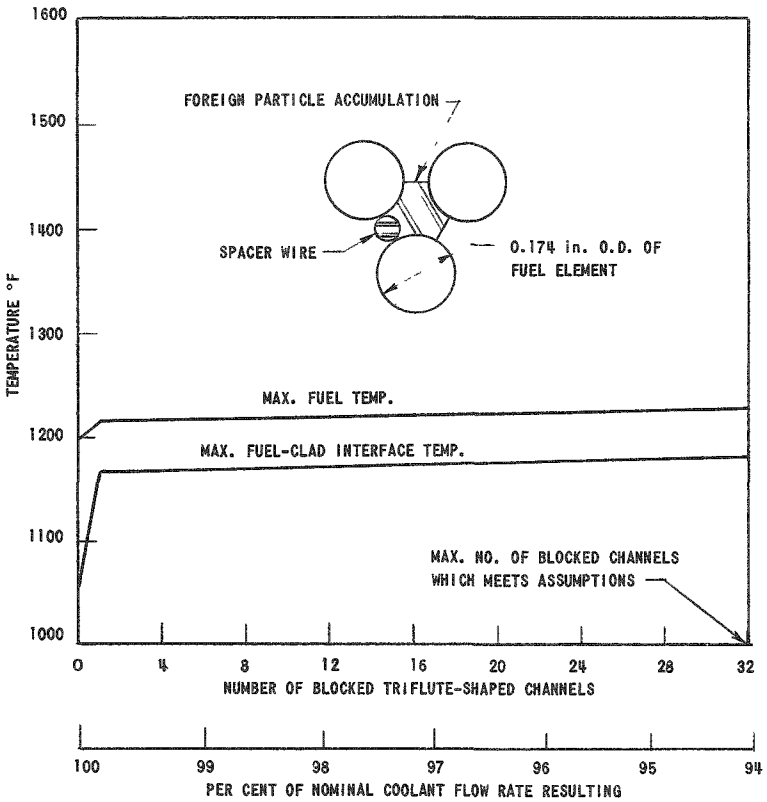

Figure 12

Foreign Particle Accumulations (Case 5) and Their Effects on EBR-II Core Temperature

6. Component Development - Instrumentation

a. Control Rod Reactivity Generator - All drawings have been completed for the original rotary design reactivity generator mechanism. However, it has been decided to investigate a linear rod oscillator reactivity generator and the rotary design has been shelved. During the dry critical experiments the control rod to be used will be calibrated by connecting it to a standard control rod drive mechanism.

The linear oscillator mechanism required for wet critical transfer function measurements is being investigated. Preliminary design calculations indicate that at 2 cycles per second a 1.5 to 1.75 hp motor would be required.

The final design of the nulling circuit for the wave analyzer has been completed and is being fabricated.

b. Neutron Source - An antimony-beryllium neutron source is being designed for EBR-II. Handling problems of a high intensity neutron source can be avoided if a satisfactory method can be devised for installation of the beryllium in the core and finally placement of the antimony into the beryllium.

All of the drawings have been completed for the inner and outer blanket positions and for the dry critical antimony storage coffin. Two stainless steel clad antimony rods which will be used during dry critical experiments have been sent to MTR-ETR for irradiation.

c. Automatic Control System - A research program was initiated to design an automatic over-all plant control for the EBR-II reactor. The design was begun by analyzing the major system components to establish which of the components would limit the over-all system response. The results obtained indicate that the currently assigned control setting of the primary system pumping rate will make the response of the primary flow system the limiting factor in over-all system control. The setting of this rate control is somewhat arbitrary, however, and if a faster primary flow response time is adopted, the reactor could be made to be the limiting piece of equipment with regard to over-all system response. Transport delays were determined for the intercomponent piping.

7. Component Development - Steam Generators

The decision to utilize two evaporators in lieu of four superheaters as an expedient and temporary means of resolving the present superheater fabrication difficulties is being implemented. A spare evaporator is now available. All material and finished subcomponents for the second unit are also available except for the tubing.

Base tubing for 100 additional mechanically bonded duplex evaporator tubes for the single evaporator to be made is in process at B&W in Milwaukee. The tubing has been hot rolled and has entered the cold drawing process. Delivery is scheduled for May 1, 1961.

Twenty assemblies are ready for shipment from ANL to the duplexing vendor to provide welding sample stock and duplex tubes to be used to set up the assembly process for this tenth evaporator unit.

Additional welding wire is being purchased and a 30 pound ingot will be vacuum cast at ANL to provide material duplicating the analysis of the wire yielding the best results in welding the first nine evaporators. This ingot will be processed to wire by a commercial vendor.

Additional experiments are being carried out to determine the feasibility of producing a satisfactory mechanically bonded superheater tube by duplexing the tubes in place in the shell, after the sodium tube-to-tube sheet welds are completed.

The expected steam temperatures which would obtain with two unmodified evaporators in lieu of four superheaters was shown in Figure 15 of the February Progress Report, ANL-6328. These steam temperatures

can be increased by increasing the effectiveness of the unit. This is accomplished by installing a central core within each tube to increase the steam velocity thus reducing the steam side film resistance which is the dominating thermal resistance.

The results of a parametric study to determine the effect of core-tube diameter on the outlet steam temperature are shown in Figure 13.

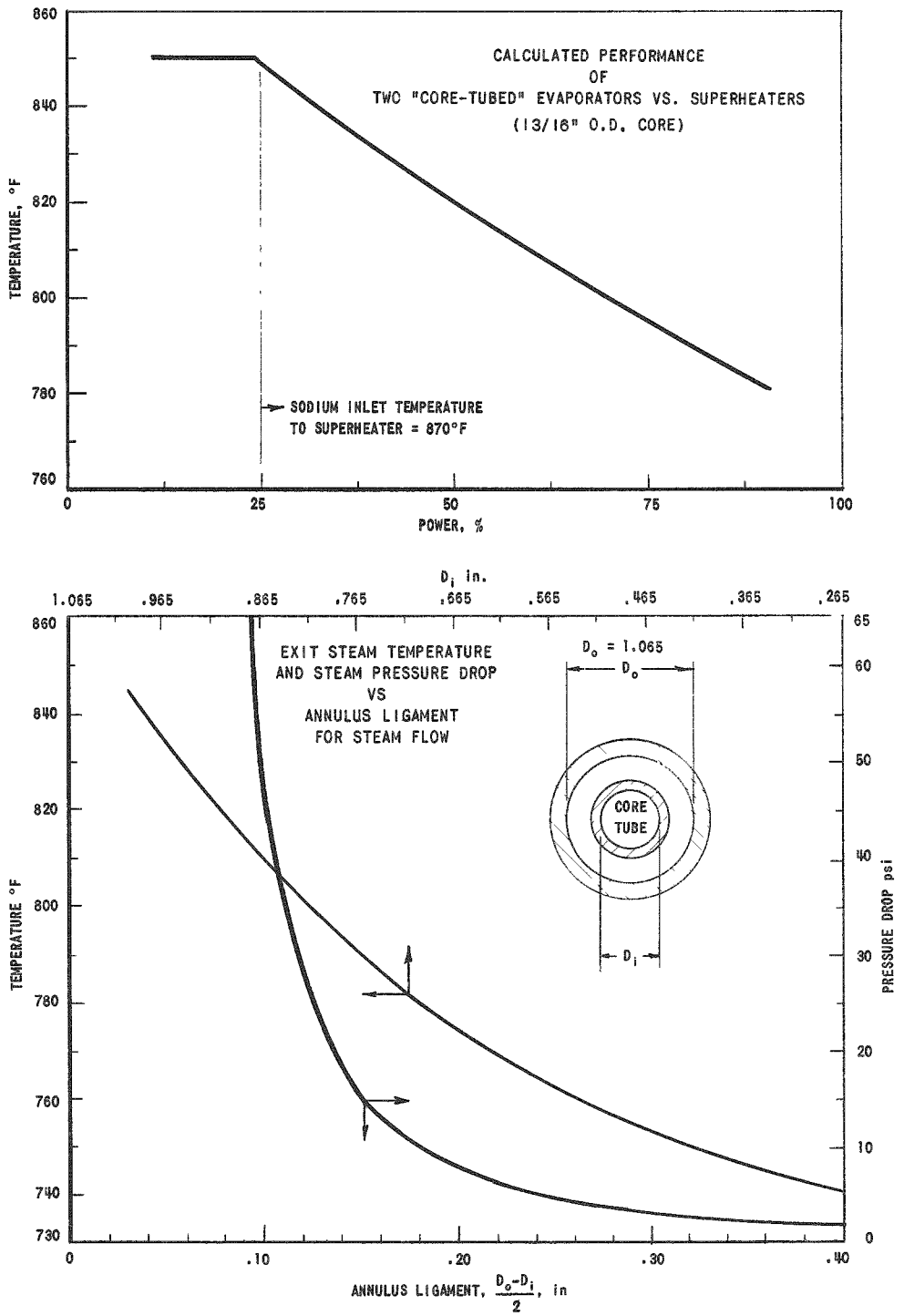

Figure 13

Core Tube Performance Characteristics

A $\frac{13}{16}$-in. diameter core will be used, giving a steam flow annulus of about $\frac{1}{8}$ in. A resulting pressure drop of about 26 psi across the steam side of the unit will be obtained. No significant change in boiler pressure is anticipated as a result of this change, since the steam piping system design was generous. At 45 Mwt the anticipated steam temperature is 790°F. A comparison of Figure 13 with Figure 15 of the February Progress Report, ANL-6328, indicates that a $\frac{13}{16}$-in. core in each evaporator tube increases the steam temperatures by 80°F to 90°F. A corresponding decrease in moisture in the final stage of the turbine and increased turbine life will be realized. Various core designs are now being studied.

8. Component Development - Fuel Reprocessing Facilities

a. Fuel Cycle Facility Design and Testing - The construction of the Fuel Cycle Facility Building is about 80 per cent completed. Installation of the cranes and manipulators in the Argon Cell has begun. The blister hoist which will be used for lifting manipulator carriages is being installed.

Component parts of two melt refining furnaces have been ordered. Two panelboards which will control the operation of these furnaces have also been ordered. High frequency inductive power will be used in the Argon Cell as a heat source in the melt refining and injection casting furnaces. Procurement of ANL supplied equipment for this installation has been completed and shipment to Idaho will soon begin.

Eight toggle switch control boxes for the control of cranes, manipulators, and blister have been returned by the manufacturer after a correction of defects which had made the switch boxes unacceptable. The switch boxes will be retested in the cell mockup.

Irradiation tests of materials which may be used in the Argon Cell continue. Fluorescent paints, useful for covering certain surfaces of cell equipment, are being tested. Some fading of the paint samples has been noted after the samples received a gamma dose of 2.7×10^8 rad.

Testing of Timken roller bearings lubricated with radiation-resistant greases continues. In the current tests, the lubricated bearings are alternately irradiated and run. The bearings have operated successfully after a total running time of 24 hours and an accumulated gamma dose of 3×10^9 rad.

b. Development of Remote Fabrication Equipment - The design of the refabrication equipment for the EBR-II Fuel Cycle Facility is estimated to be 73% complete. During the reporting period the design work was completed on the depalleting, fuel pin processing and inspection machines.

The drawings are being checked and bills of materials and specifications are in preparation. The installation drawings, including electrical and pneumatic control diagrams, are approximately 30% complete and prefabrication of electrical controls is approximately 15% complete.

Completion of Core I fabrication has allowed the testing of equipment and process development to be accelerated. Work which is rapidly approaching completion includes the testing of differential pulse-type, eddy current sodium bond and level detectors. It has been found that this equipment produces much more easily read and more reliable indications of sodium level than the Cyclograph and is about equally satisfactory in the detection of bond voids.

Eddy current tests were also run on fuel elements at room temperature and again at temperatures between 100 and 150°C. At room temperature, the sodium level is in the solid state and the gas-metal interface was deeply indented by shrinkage. The eddy current signal from this interface was of poor resolution. In spite of the attempts to obtain a directional solidification of the sodium, the annulus between the fuel pin and tube contained many inconsequential shrinkage voids, which were shown as rejectable voids by the eddy current tests. With the sodium in the molten condition, the sodium level was more regular and the shrinkage voids did not exist to confuse the test signal. Changes in temperature resulted in a base line shift of the Cyclograph but did not greatly affect the signal from the differential pulse eddy current tester.

A chassis was mocked up to test the modular plug-in principle used in the pin processing station. This chassis included the locating devices, pneumatic connectors, electrical connectors, and manipulator operated locking slides all of which are integrated in the subchassis and installed and connected as a unit to the machine base by manipulator. The feeder and delivery cams for the depalleting station were mocked up and tested.

Fuel subassemblies from the EBR-II reactor core will be cut open with the fuel dismantler to remove the fuel elements for subsequent decanning operations. A non-operational model of the dismantler was built to study spatial and functional arrangements of the various components. In conjunction with this model, master-slave manipulators will be used to perform and evaluate the necessary remote adjustment and maintenance operations.

An experimental device for removing the fuel elements from their grid support has been constructed and tested. Modifications are currently being incorporated to improve its performance before designing a prototype.

The design of some components has been developed to the stage where prototypes can be fabricated. The main support beam has been designed to permit considerable freedom in positioning the individual components so that the most appropriate positions can be established in the final prototype assembly. In case it is impossible to pull the hexagonal tube off the fuel and blanket elements, a slitter is being fabricated which will cut the tube longitudinally. A fuel subassembly rotational drive has also been designed for prototype use.

9. Process Development

a. Melt Refining Process Technology - A third small-scale melt refining experiment with highly irradiated fuel has been completed. This run is one of a series of runs that is being made to determine the optimum conditions for the melt refining of irradiated fuels. The formation of an excessively large amount of skull material during the experiment has led to a re-evaluation of the melt refining procedure used in laboratory studies. A change in the environment of the pins during storage periods preceding melt refining experiments has been proposed as a means by which the amount of oxide formed by extraneous reactions may be reduced.

In the present run, a 360-gram charge of ten per cent enriched uranium-five per cent fissium, irradiated to an estimated burnup of one total atom per cent and cooled for 14 days, was melt refined for one hour at 1400°C. The shorter holding time (previous holding times were three hours) was employed to test the effect of radiation on the pouring yield. If the increased amounts of oxide found in the preceding runs with irradiated fuel resulted from a radiation-induced increase in the rate of reaction of the uranium with the crucible, the shorter holding time in the present run should have resulted in the production of a smaller amount of oxide and a higher pouring yield. Instead, a yield of about 52 per cent was obtained, and considerable evidence of reaction of uranium with oxygen and nitrogen was apparent in a visual examination of the skull material.

In all the runs with unirradiated and irradiated fuel, the pins were stored in a zirconia crucible in the melt refining furnace before being melt refined. During the storage period (69 hours in the present run and shorter periods in preceding runs) the furnace containing the pins was subjected to continuous evacuation. The temperature of unirradiated pins during storage was about 25°C. In the present run, because of fission product decay heat, the temperature of the pins during the 69-hour storage period varied between 350° and 375°C. In this temperature range, oxidation and nitridation rates are high, and even a slight decrease in vacuum efficiency, either through in-leakage or back diffusion from the pumping system, may provide an undesirably large source of oxygen and nitrogen. The presence of "pinshells" in the skull material indicates that air leakage did occur.

It should be noted that the conditions prevailing during the laboratory runs do not entirely simulate the conditions envisioned for the runs in the EBR-II Fuel Cycle Facility, where the entire procedure will be carried out in an argon atmosphere.

The information obtained from the present melt refining experiment prescribes an important change in the melt refining procedure for laboratory runs with irradiated material. Because of the high temperatures that are attained by the pins through fission product decay heating, it is essential that contact of the pins with air be prevented during storage periods. Since the problems of providing a reliable leak-proof furnace system seem excessively difficult by comparison, the more practical solution appears to be the employment of a static system in which an inert atmosphere, preferably under a slight positive pressure, is maintained in the furnace system during the storage period.

Experimental work was completed on the nitridation rates of unirradiated, sodium-coated fissium pins in argon-nitrogen mixtures. This information is of interest since declad fuel pins will be handled in the argon atmosphere of the Fuel Cycle Facility, which is expected to contain small concentrations of nitrogen. The nitridation rate was constant with increasing nitrogen concentrations above about five per cent. As the nitrogen concentration was decreased below this level, the rate of nitridation dropped markedly.

A Fiberfrax cover on the melt refining crucible is employed to collect volatilized sodium. A brief study of the chemical reaction involved indicates that it resembles a basic fusion of silicate.

b. Processing of Melt Refining Skulls - The skull reclamation process involves removal of a melt refining skull by oxidation to convert it to a powder, selective extraction of noble metals from a chloride flux-oxide slurry into zinc, reduction of uranium oxides by magnesium in a zinc solution, two uranium precipitations to permit removal of fission products in supernatant solutions, and a retorting step to isolate a uranium metal product.

Demonstration runs of the skull reclamation process with 400-gram-uranium charges are being continued. Fission product removal data have now been obtained for the two demonstration runs reported in the February Progress Report (ANL-6328). The data show that removals of cerium, molybdenum, and palladium were adequate, whereas the removals of ruthenium and zirconium were inadequate. However, noble metal extraction by zinc at 800°C was not employed in these runs, and its incorporation into the skull reclamation process should result in a marked improvement in ruthenium separation. The relatively low (about 50 per cent) removal of zirconium requires further studies.

Additional demonstration runs were made during March, one of which incorporated the noble metal extraction step. In the noble metal extraction step, separation of phases was readily accomplished by pressure-siphoning off the liquid zinc phase after solidification of the salt. Ninety-two per cent of the zinc was transferred. Analysis showed that the zinc phase contained only 0.4 per cent of the uranium charged. This procedure is considerably more promising than transfer of the flux-oxide slurry because of the difficulty of keeping the oxide in suspension in the flux. Data are not yet available for evaluating the removal of fission product elements.

Information is being obtained on uranium and fission product behavior in zinc solutions of high magnesium concentration (near 50 weight per cent). This system is employed in both the blanket and skull reclamation processes. The uranium solubility can be reduced to 0.1 per cent or below by cooling to about 400°C. Ruthenium precipitates or coprecipitates with the uranium. The cerium concentration (initially at 0.2 per cent) is unchanged on cooling.

Refractory zirconium oxide, which is found in the oxidized melt refining skull as crucible fragments, is not reduced significantly by the zinc-magnesium solution used for the reduction of uranium oxide. This zirconium oxide is expected to remain in the flux phase during the reduction.

The agglomeration of uranium precipitated from high magnesium-zinc systems into large masses is desirable for product handling purposes. High temperature (about 800°C) and good agitation seem to promote agglomeration.

c. Plutonium Recovery Processes - Experiments to determine the feasibility of separating plutonium (and uranium) from rare earth metals by making use of the known insolubility of the former in calcium are being continued. Calcium alloyed with zinc, rather than calcium alone, is being used in these studies. The solubility of uranium at 725°, 750°, and 775°C in calcium-zinc mixtures containing up to 31 per cent calcium have been determined. Plutonium-cerium separations were not obtained in this composition range. The solubility of plutonium was found to be considerably greater in the calcium-zinc system than the solubility of uranium. In a 31 weight per cent calcium-zinc mixture at 750°C, the solubility of uranium was 6×10^{-4} weight per cent, whereas the solubility of plutonium was 0.30 weight per cent. Additional studies are being conducted at higher calcium concentrations.

d. Liquid Metal Reduction Studies - Uranium tetrafluoride was reduced quantitatively to uranium metal by a zinc-five weight per cent magnesium solution in less than 10 minutes at 750°C. A calcium chloride-magnesium chloride-magnesium fluoride flux was used.

e. Materials and Equipment Evaluation - Zinc vapor was found to penetrate CS grade graphite, and the material, therefore, is considered unsuitable for process use. Grades of graphite of greater density will be tested. Preliminary tests of pyrolytic graphite and dense magnesia in zinc at 850°C indicate that these materials may be useful, but further evaluation is needed. Testing of refractory metals (tantalum, molybdenum, tungsten, and tantalum-tungsten alloys) is also in progress. A vapor-deposited tungsten coating on 446 stainless steel showed good adherence after eight thermal cycles between 100° and 800°C despite the relatively large difference in thermal expansion coefficients of these materials.

Construction of a large-scale cadmium distillation unit is nearly completed. This unit will be used to demonstrate, on an engineering scale, distillation and various liquid metal handling operations.

10. Fuel Development and Fabrication - Core I

a. Fuel Element Production - The manufacture of the Core I fuel rods has been completed, and the required number of fuel elements have been constructed (except for 3 boron-carbide safety elements). The summary of the process yield for 10,500 fuel rods discloses that 8.23% were rejected for bonding defects giving a bonding yield of 91.7%. The over-all yield for the process was 76.2%.

b. Fuel Prototype Irradiation - The prototype irradiation sample CP-5-21 was loaded into CP-5 during the latter part of February. The approximate maximum control metal temperature is 620°C to 650°C (1150°F-1200°F). The irradiation of this sample is proceeding satisfactorily and it will be continued until the sample achieves 2% burnup.

c. Reaction Rate of Uranium and Stainless Steel - Safety considerations for EBR-II Core I operation require information about the rate of penetration of Type 304 stainless steel jacketing by molten fuel. To that end a technique has been developed based on immersing capsules of desired wall thickness into the molten fuel. Inside the capsule is an insulated wire which is shorted when the molten alloy breaks through the stainless steel wall thus giving an indication on a high speed recorder. Penetration studies of molten uranium in the temperature range 1150° and 1350°C have been made using 0.010 in. and 0.040 in. wall Type 304 SS capsules. The preliminary data are given in Table IV. Check runs showed that the time to penetrate 0.040 in. wall capsules was very reproducible while the 0.010 in. wall capsule data had some scatter. This can be attributed to greater nonuniformity in the wall thickness of the thin capsules.

Table IV. Time (sec) to Penetrate 0.010 and 0.040 in. Wall 304 Stainless Steel by Molten Uranium

Temp. (°C)	0.010 in.	0.040 inch
1148	0.4	2.7
1187	1.9	11.5
1244	1.7	9.5
1300	-	9.0
1350	-	6.3

As can be seen from the data, it takes about 4 to 5 times as long to penetrate the stainless steel at 1187°C than it does at 1148°C for 0.010 in. as well as for 0.040 in. wall capsules. This slower rate of penetration at a higher temperature was unexpected. The possibility that heavier surface films at higher temperatures slow down the rate of penetration is negated by the thin and thick wall capsule test results. The tendency for the austenitic structure of Type 304 stainless steel to transform to ferrite in this temperature range is being studied as a possible explanation of this anomaly.

A study of penetration of 304 stainless steel by U-5 w/o Fs is now under way.

11. Core II Fuel Development

a. Fast Reactor Fuel Jacket Development - A remelted ingot of niobium-chromium and a quantity of niobium alloy strip stock was received from Battelle during March. This material will be used in development work on the fabrication of tubing for EBR-II Core II.

b. Casting and Jacketing Technology of U-Pu-Fs Fuel Pins - Twenty-one of the 2 in. long specimens, described in previous reports, were jacketed and sodium bonded into niobium, Nb-1 w/o Zr, vanadium, Inconel-X and Type 304L stainless steel jackets for irradiation testing. A 0.0005 in. thick vanadium barrier foil was used between the fuel and the Inconel-X and stainless steel jackets. To prevent external alpha contamination of the jackets, a disposable, polyethylene loading funnel was inserted into the jacket tubes and the plutonium-containing specimens were dropped through this funnel onto the sodium at the bottom of the tubes. The sodium was melted and an extended plug was inserted into the top of the jacket and fusion welded to the tubes by the inert-gas-shielded, tungsten-arc process. Satsifactory welds were produced with each of the materials described.

The specimens were then surveyed for contamination. One specimen required decontamination. Leak detection was accomplished by the mass spectrometer method and all specimens were bonded at 400°C for 30 seconds in a machine which imparted a mechanical shock at a rate of 30 shocks per second to the bottoms of the specimens.

X-ray and eddy current inspection showed an improper sodium level in two specimens, a displacement of the vanadium barrier foil in one of the stainless steel jacketed specimens, and a bond void in one specimen. Since these specimens were properly identified and represented typical types of fuel element defects, it is felt that useful information may be obtained by the irradiation of the defective as well as of the properly assembled and bonded fuel specimens.

12. Dry Critical Experiments

The Dry Critical Program is summarized on page 44 of ANL-6238. These experiments will be conducted with no liquid metal coolant in the primary system. Therefore, the following special restrictions have been established with respect to both power level and temperature throughout the conduct of the dry critical experiments:

(1) Temperature of components in the primary system shall not exceed 120°F at any time.

(2) Fuel element clad temperature shall not exceed 180°F at any time.

(3) Reactor power level shall not exceed 1 kw at any time. Steady-state operation will be between 5 and 50 watts.

The first restriction is necessary to avoid overheating of fission counters and ion chambers for monitoring neutron flux. The second restriction is made to prevent melting of fuel element bond sodium during the dry critical program. The third restrictions are to permit extended periods of operation without excessive activation of fuel alloy.

To achieve these objectives it is necessary to relate accurately the reactor power level to the nuclear instrument (fission counter) response. This will provide a basis for determining power level trip settings as well as for monitoring the reactor power level. The pre-experimental calibration is determined by extrapolating from the data obtained on the EBR-II mockup on ZPR-III, as well as by purely theoretical prediction. It was found that the two methods differ by less than 20% in determining the total reactor power as a function of fission counter response in or near the reactor core. Therefore, it is possible realistically to monitor the reactor power level during the dry critical experiments without a detailed measurement of the power distribution.

III. STUDIES AND EVALUATIONS (040116)

A. Plutonium Value Studies

A study is being made of plutonium values based on the fast reactor data presented in ANL-6212.* This study compared the plutonium-fueled reactor cases presented with comparable cases where the only change was to substitute U^{235} fuel for the plutonium. Plutonium production rates were set up based on the neutron balances given in the reference report. Assuming that unit fuel cycle costs are identical for uranium and plutonium-containing fuels, a value for plutonium can be determined by comparing uranium and plutonium-fueled systems of like core volume and composition.

The cases studied had core volume, fissile material, fuel clad material, and fuel form (either metallic, oxide, or carbide) as parameters. In the case where the initial fissile material was U^{235}, it was assumed that all plutonium was recovered for sale and all fissile makeup in the core was with U^{235}. Where the core feed plutonium was pure Pu^{239}, any core fissile makeup was from the plutonium formed in the blanket. Where the core feed plutonium was other than pure Pu^{239}, it was assumed that all plutonium formed in the blanket was sold and all core makeup was the same outside plutonium source as the initial "low quality" plutonium.

With the assumptions made on fuel cycles, the significant cost variables were the value or price of any makeup fissile material, the rental charge of fissile material in inventory and the value of plutonium sold. The value of plutonium was determined by having the net income (sale of plutonium less the purchase of makeup fissile material and fissile rental charge) from like systems equal. By equating the net income from a U^{235}-fueled case to a Pu^{239}-fueled case of like core volume and composition, a value of Pu^{239} could be obtained for any assigned price of U^{235}. Then, by using this value of Pu^{239} for blanket-produced plutonium in cases where the core feed was so-called "low quality" plutonium, a value for the "low quality" grade could be determined.

Table V lists the values of plutonium determined in these preliminary calculations using the ANL-6212 data which are for initial rather than equilibrium conditions. The assigned U^{235} price was \$17/gm of U^{235}, the assumed system inventory was 1.5 times the critical mass given in ANL-6212 and the fissile rental charge was 4%. The fuel clad was iron and the coolant was sodium.

---

*S. Yiftah and D. Okrent, "Some Physics Calculations on the Performance of Large Fast Breeder Power Reactor," ANL-6212 (December 1960).

Table V. Plutonium Values

Core Volume (liters)	Fuel Form	Pu Value - $/gm Fissile[1]		
		Pu-A Feed[2]	Pu-B Feed[3]	Pu-C Feed[4]
800	Metal	31	39	65
	Oxide	28	31	36
	Carbide	29	32	41
1500	Metal	30	51	104
	Oxide	27	31	37
	Carbide	28	33	44
2500	Metal	30	62	101
	Oxide	27	31	39
	Carbide	27	35	51

[1] Fissile plutonium assumed to be Pu^{239}, Pu^{241} only.

[2] Pu^{239} - 100%.

[3] Pu^{239} - 75%; Pu^{240} - 10%; Pu^{241} - 12%; Pu^{242} - 3%.

[4] Pu^{239} - 40%; Pu^{240} - 10%; Pu^{241} - 25%; Pu^{242} - 25%.

The results are preliminary and are indicative only of a possible direction. This direction can be stated as follows: insofar as fast reactor systems are concerned, the value of plutonium, regardless of isotopic composition, is at least as high as any price set for uranium.

IV. REACTOR SAFETY (040117)

A. Thermal Reactor Safety Studies

1. Fuel-coolant Chemical Reactions

Knowledge of the nature and extent of chemical reactions with nuclear reactor core metals that may occur in pressurized water or steam is essential to safe operation of reactors. The principal laboratory procedure uses a condenser discharge to provide almost instantaneous heating and melting of metal wire in water or steam. The energy input to the wire indicates reaction temperature; the transient pressure measures reaction rate; light emission indicates time-temperature behavior; hydrogen generated gives extent of reaction, and particle size of the residue indicates the surface area exposed to reaction. A second method consists of heating the metal inductively and then subjecting it to a steam pulse to induce a metal-steam reaction.

The reaction of stainless steel with uranium oxides is being studied by use of differential thermal analysis

Studies of the kinetics of metal-water reactions under reactor incident conditions are being made in the TREAT reactor.

The series of zirconium runs in room temperature water in the large reaction cell are continuing Four runs with initial metal temperatures in the melting point region (1840°C) have shown some increased reaction. More runs will be required to determine if the increase is significant

Studies of the aluminum-water reaction by the pressure-pulse method are continuing Contact time between the one-atmosphere steam and the molten aluminum has been extended to 1000 seconds. Runs at 1000° and 1200°C show only very slow reaction

Differential thermal analyses were made with pressed mixtures of stainless steel and 10% of either UO_2 or U_3O_8 These unfired fuel pins were heated to 1200°C at the rate of 10°C per minute in an argon atmosphere. No exothermic reaction was noted. X-ray diffraction analyses of the mixtures before and after heating indicated that the U_3O_8 was reduced to UO_2 and that the UO_2 was not reduced

Theoretical calculations (on the analog computer) of the zirconium water reaction are based on the assumption that subcooling of the water results in a decreased rate of diffusion of water vapor through the hydrogen film surrounding reacting particles. It follows from this that increased reaction would occur in a reaction cell having increased vapor volume and

that a decreased reaction would occur in the presence of added inert gas. Detailed comparisons between computed and experimental data are in progress.

The eleventh series of TREAT, metal-water meltdown tests was completed. Cermet fuel plates of 90 w/o SS-304, 10 w/o UO_2, 93% enriched, gave 5.2, 9.1, and 11.0 per cent reaction of the molten stainless steel with water for reactor bursts of 368, 490, and 495 megawatt-seconds respectively (51 millisecond period). These amounts of metal-water reaction are slightly higher than previous results with SS-UO_2 cermet pins. It is concluded, therefore, that the influence of initial fuel geometry is not of major importance in determining the extent of metal-water reaction for these cermet fuels. It was observed that segregation of the UO_2 away from the SS-304 takes place during the transient.

2. Kinetics of Oxidation and Ignition of Reactor Materials

Studies are being made of the oxidation and ignition kinetics of the metals uranium, zirconium, and plutonium in order to provide information leading to an understanding of the reactions. This knowledge should make it possible to minimize the hazards associated with handling these nuclear reactor materials. Isothermal oxidation on microscope stage, shielded ignition, burning curves, rate of propagation of burning foil, and burning temperatures are the techniques being used. In the continuing study of ignition and burning of uranium, zirconium, and plutonium, more emphasis is being placed on the burning process. Burning propagation rate studies provide a useful tool to observe the effects of many variables.

Studies of the relationship between isothermal oxidation rates and burning curve ignition temperatures are continuing. Calculations of the burning curve were made for a high specific area uranium sample. The calculated results, however, deviate from experimental results and further study is required.

Studies of burning propagation along foil strips are continuing. Construction and calibration of a two-color photoelectric pyrometer was completed. It is now possible to measure both the maximum temperature and the propagation rate of burning along metal strips with one instrument.

Ignition temperatures and specific areas were measured for uranium monocarbide powder fractions from different sources. Comparisons based on mesh sizes alone were not significant because of differences in roughness factors. Estimates of the true specific areas of -270 +325 mesh powders were made by Armour Research Foundation using a Fisher Sub-Sieve Sizer. Samples having different roughness factors were then correlated on the basis of their specific area. Uranium monocarbide powders were not

as pyrophoric as uranium powders of similar specific area. Uranium monocarbide ignition temperatures were about 40 degrees higher than uranium. For example, at -230 +270 mesh, uranium monocarbide powder ignition occurred at 290°C compared with 250°C for similarly sized uranium powder.

B. Fast Reactor Safety Studies

1. Stability of Fast Reactors: Calculation of Oscillating Temperatures in EBR-II

The "radially lumped" pin temperature model discussed in the February Progress Report leads to the following expression* for the oscillating temperature $T_c(z)$ in the coolant for a heat source $a(z)$ per unit length of pin:

$$T_c(z) = T_c(o)\, e^{-\frac{\lambda z}{v}} + \frac{e^{-\frac{\lambda z}{v}} \int_0^z a(z')\, e^{\frac{\lambda z'}{v}}\, dz'}{\lambda h \tau_c (1 + i\omega\tau_f)} \qquad (1)$$

where:

h is an overall heat transfer coefficient defined so that $h(\bar{T}_1 - T_c)$ is the total heat transferred per unit length of pin, T_1 being the "lumped" fuel temperature.

v is coolant velocity

ω is frequency, radians/sec

$\tau_c = \frac{C_c}{h}$, where C_c is heat capacity of coolant per unit length.

τ_f is a fuel pin time constant, which represents the ratio of heat stored in the pin per unit temperature rise of the fuel to heat lost per unit temperature difference between fuel temperature and coolant temperature. This is related to the ratio of the average fuel temperature (relative to T_c) to the temperature at the outside of the pin (relative to T_c), and this ratio is contained in the constant h, which can be defined as

$$h = 2\pi R h_F \frac{T(R) - T_c}{T_1 - T_c} \qquad (2)$$

where R is the outer radius of the pin and h_F is the coolant film heat transfer coefficient.

---

*F. Storrer, "Temperature Response to Power, Inlet Coolant Temperature and Flow Transients in Solid Fuel Reactors," APDA-132, June 5, 1959.

Storrer's development was for an unclad fuel pin, and for this case

$$\frac{1}{h} = \frac{1}{8\pi k} + \frac{1}{2\pi R h_F} \tag{3}$$

where k is the thermal conductivity of the pin. τ_f is given by C_1/h, where C_1 is the heat capacity of the pin per unit length. λ is then given by

$$\lambda = \frac{\omega}{1 + \omega^2 \tau_f^2} \left[\frac{\tau_f^2}{\tau_c} \omega + i \left(1 + \frac{\tau_f'}{\tau_c} + \tau_f^2 \omega^2 \right) \right] \quad . \tag{4}$$

The EBR-II pin must be treated as having two radial regions, a fuel region 1, and a homogenized bond and clad region 2. In this case Equation (1) still applies, but it is necessary to modify the definition of λ to the following:

$$\lambda = \frac{\omega}{1 + \omega^2 \tau_f^2} \left[\frac{\omega \tau_f \tau_f'}{\tau_c} + i \left(1 + \frac{\tau_f'}{\tau_c} + \omega^2 \tau_f^2 \right) \right] \tag{5}$$

in which

$$\tau_f = \frac{C_1 + C_2 [(T_2 - T_c)/(T_1 - T_c)]}{h} \tag{6}$$

$$\tau_f' = \frac{C_1 + C_2}{h} \tag{7}$$

and h is found from (2) by using the two region steady-state temperature solution with a constant heat source in region 1, rather than by using (3).

These developments are based on the assumption that any difference between the pin temperature and the coolant temperature at a height z is due to the local heat source a(z). They do not really apply to calculations of amplitude attenuation with no source present. In such a case a reasonable alteration of the lumped model is to set $\overline{T}_1 = \overline{T}_2 = T(R)$, so that $\tau_f = \tau_f'$ and $h = 2\pi R h_F$. This corresponds to a radially constant temperature in the pin but allows a temperature difference between coolant and pin which would not be present in the steady state. The accuracy of this assumption has not been tested, however.

It has been found in studies of the EBR-II feedback that phase shifts are very nearly linear in ω up to 5 radians/sec. This is to be expected when typical values of constants for EBR-II are examined for a coolant velocity of 537 cm/sec, the average full flow value. In this case $\tau_f = 0.104$ sec, $\tau_f' = 0.136$ sec, $\tau_c = 0.0410$ sec, $\tau_f'/\tau_c = 3.32$

$$\frac{z}{v} = \frac{36.12}{537} = 0.0672 \text{ sec (for full height of core)} \quad .$$

λ for low frequency is approximately

$$i\omega\left(1+\frac{\tau_f'}{\tau_c}\right)$$

the terms in ω^2 being small. The coolant transport lag in the core is of the order of $\omega[1 + (\tau_f/\tau_c)]\, z/v$ which, for $\omega = 1$, is 0.29 sec. Lags in the EBR-II core and upper coolant gap are thus of the order of tenths of a second.

They are slightly longer in the upper blanket, but the reactivity contribution there is small.

Equation (1) with λ as given by (5) was used in a calculation in which four axial sections were used in the core. Table VI shows this result compared with results of an IDO-102 calculation for the outlet temperature of the core for a 1% oscillation at full power.

Table VI. EBR-II Coolant Temperatures at Core Outlet Relative to Power for 1% Full Power Oscillation

(Full Flow: 537 cm/sec Average Velocity)

	Amplitude, °C		Phase	
ω, radians, sec	Eq. 1	IDO-102	Eq. 1	IDO-102
	V = 270 cm/sec			
0.1	2.721	2.824	- 2.4°	- 2.4°
1.0	2.599	2.713	-22.7°	-23.3°
2.5	2.100	2.228	-52.7°	-55.0°
5.0	1.248	1.316	-84.9°	-92.3°
	V = 537 cm/sec			
0.1	1.579	1.376	- 1.5°	- 1.5°
1.0	1.545	1.352	-14.8°	-14.4°
2.5	1.387	1.271	-35.3°	-35.2°
5.0	1.033	0.953	-61.5°	-62.4°
	V = 786 cm/sec			
0.1	0.929	0.929	- 1.1°	- 1.2°
1.0	0.916	0.918	-11.5°	-11.5°
2.5	0.852	0.898	-27.7°	-28.4°
5.0	0.691	0.714	-49.7°	-51.2°

2. Core Meltdown Studies: TREAT Program

In-pile meltdown experiments are being performed in the TREAT reactor in order to survey types of fast reactor fuel element failure and the associated movement of fuel element materials, as well as to determine the mechanisms producing such phenomena.

a. EBR-II, Mark-I Dry Samples - A total of seven, 3% enriched EBR-II Mark-I elements contained in special capsules to shape the sample power axially have been examined after irradiation in TREAT. Results of the examination of the first sample, which did not suffer failure, confirmed the predicted power profile and were reported in the February Progress Report. In addition, the remaining three samples of this series of experiments surveying the effects of an axial "chopped cosine" power shape, were run at TREAT and are being shipped back for examination. All of the first eight capsules were subjected to power transients initiated with a period of 110 milliseconds and scrammed at predetermined values of reactor energy release. The last two were given flattened reactor power bursts of about 2.5 sec.

Results of the post-mortem examination of the six elements which failed were consistent with previous results on similar elements which were subjected to an essentially constant axial power profile; each element failed in the central region. A typical result is shown in Figure 14.

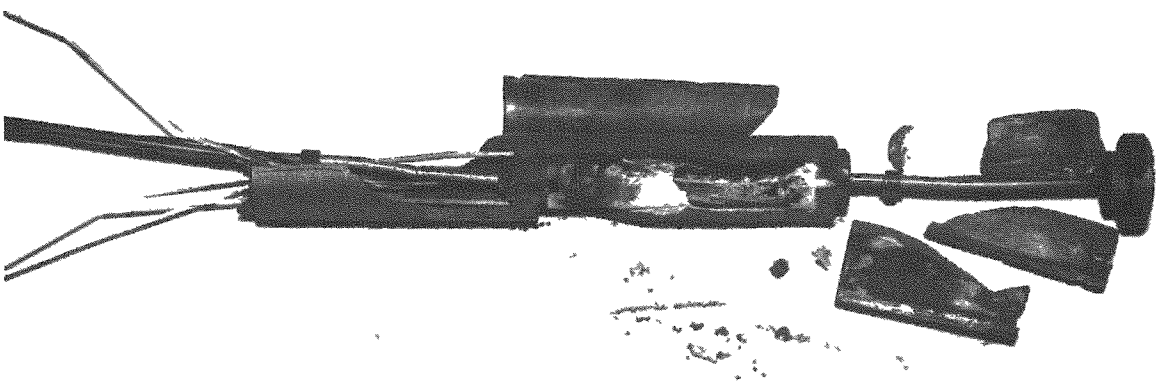

Figure 14

Sample EBR-II Mark I Pin after TREAT Exposure

The fuel alloy was found to have been expelled upwards from the bottom portion of the element, and downwards from the top portion, with essentially all the fuel distributed within a length of crucible of about 18 cm. A small cylinder of fuel alloy about 1.5 cm long (presumably from one end of the element) was found among the spattered meltdown residue for a sample given an energy input approximately 20% greater than that estimated to be sufficient to cause "extensive failure" in the central part of

the sample. As the total energy input of the samples examined was increased, the amount of cladding remaining decreased and, for an input of about 70% greater than that necessary for extensive failure, only about one-half of the cladding remained.

b. Development of Samples with Internal Thermocouples - One natural enrichment EBR-II element containing a tantalum-sheathed, tantalum-molybdenum thermocouple has been prepared for a series of three, progressively more severe, transient experiments in order to test in-pile this technique of sample temperature measurement. The element thermocouple has been calibrated and is being shipped to TREAT.

c. EBR-II, Mark-I Elements in Stagnant Sodium - The four 3% enriched EBR-II, Mark-I elements encapsulated in stagnant sodium (see February Progress Report) shipped to TREAT at the close of the last report period were run as planned. They have been sent back, but not yet examined. Temperature records from these experiments will be compared against the post-mortem results for guidance in future thermocouple instrumentation of EBR-II and Fermi-I elements contained in a sodium bath.

d. Irradiated EBR-II Fuel Rods for TREAT Tests - Four NaK capsules, each containing three reference U-Fs alloy fuel pins jacketed with 304 stainless steel and bonded with sodium, have been returned after being irradiated in the MTR. The four capsules, ANL- 42-50, 53, 54 and 56 are part of the series ANL- 42-50 through 57 which will provide irradiated EBR-II rods for tests in the TREAT reactor. The TREAT tests will simulate excursions on rods which have already been irradiated.

The four capsules have been opened, the rods examined, and dimensions and immersion volumes taken of the clad fuel for the purpose of providing information additional to that from the TREAT tests. The in-pile operating conditions and performance data are given in Table VII. The examination revealed all twelve rods to be in excellent condition with no gross changes evident. The data indicate successful operation up to 1.5 a/o burnup at fuel core temperatures of 590°C; bulk volume increases of about 0.3% were noted. On a projected basis, the data indicate excellent stability of EBR-II fuel rods in the temperature range 400 to 590°C with volume increases of less than 1% ΔV per a/o burnup to be expected.

Only two of the rods indicated a change in diameter. One showed a decrease of 0.002 inch and the other an increase of 0.002 inch, both values being close to the precision of the measurements which was $\pm$ 0.001 inch. Although the data suggest no change in diameter of the rods, when considered in conjunction with the volume data, the probability of an increase in diameter of something less than 0.001 inch on most of the rods is indicated.

Table VII. Irradiation Data on U-Fs and U-Fs-Zr Fuel Alloys

Capsule	Rod Number	Composition[a] w/o Fs	Zr	Max. Fuel Temp. °C	Max. Jacket Surface Temp. °C	Max. Heat Flux[b] BTU/hr-ft^2	Burnup[c] a/o	Weight Change, mg	Diameter Change[d] %	Bulk Volume Change[e] %	% Volume Change a/o BU
ANL-42-53	ET2-2	5	2.5	590	560	600,000	1.5	-10.7	NMC	+0.26	+0.17
ANL-42-53	ET2-4	5	2.5	590	560	590,000	1.5	-28.9	NMC	+0.26	+0.17
ANL-42-53	ET2-5	5	2.5	590	560	600,000	1.5	-16.0	NMC	+0.35	+0.23
ANL-42-54	ET2-6	5	2.5	540	510	540,000	1.4	+ 4.2	NMC	+0.26	+0.19
ANL-42-54	ET2-7	5	2.5	540	510	540,000	1.4	-13.3	NMC	+0.26	+0.19
ANL-42-54	ET2-8	5	2.5	540	510	540,000	1.4	-12.8	NMC	+0.26	+0.19
ANL-42-56	ET1-4	5	-	580	550	590,000	0.58	- 6.4	-1.1	+0 25	+0.43
ANL-42-56	ET1-5	5	-	580	550	590,000	0.58	-25.5	NMC	NMC	-
ANL-42-56	ET1-6	5	-	580	550	600,000	0.58	-25.0	+1.2	NMC	-
ANL-42-50	ET2A-2	5	2.5	400	380	390,000	0.36	- 2.1	NMC	+0.26	+0.72
ANL-42-50	ET2A-5	5	2.5	400	380	390,000	0.36	- 6.7	NMC	NMC	-
ANL-42-50	ET2A-13	5	2.5	400	380	390,000	0.36	-20.6	NMC	NMC	-

[a]Balance is uranium.

[b]Based on outer surface of the jacketed assembly.

[c]Percent of total core atoms fissioned based on an analysis of cobalt flux monitors.

[d]NMC means no measurable change within the precision of the measurements which is ±0 001 inch.

[e]NMC means no measurable change within the precision of the measurements which is ±0.013 cc.

Slight warpage prevented an accurate measurement of the length of each rod. The results obtained using a ruler, although not accurate, indicated no detectable change in length.

A comparison of the pre- and postirradiation bulk densities is given in Table VIII.

Table VIII. Comparison of Pre and Postirradiation Bulk Density Measurements

Rod Number	Composition[a] w/o Fs	Zr	Bulk Density, g/cc Pre	Post	Change[b]
ET2-2	5	2.5	11.50	11.47	-0.03
ET2-4	5	2.5	11.46	11.43	-0.03
ET2-5	5	2.5	11.42	11.38	-0.04
ET2-6	5	2.5	11.53	11.50	-0.03
ET2-7	5	2.5	11.54	11.51	-0.03
ET2-8	5	2.5	11.42	11.39	-0.03
ET2A-2	5	2.5	11.55	11.52	-0.03
ET2A-5	5	2.5	11.21	11.20	-0.01
ET2A-13	5	2.5	11.18	11.16	-0.02
ET1-4	5	-	11.85	11.82	-0.03
ET1-5	5	-	11.71	11.69	-0.02
ET1-6	5	-	11.74	11.73	-0.01

[a]Balance is uranium.

[b]A change of ±0.02 g/cc falls within the precision of the measurements.

Volume changes were determined by immersion under the assumption of no weight change in the specimen. The data indicate a slight increase in the bulk volume of the specimens which is very close to the precision of the measurements, i.e., ±0.013 cc.

The remainder of the capsules in the series has been discharged from the MTR and is being returned for disassembly and examination.

3. Component Development

a. Small Sodium Loop - The estimates of the status of the small sodium loop as of March 21, 1961, are as follows:

Description	Estimated % Completion
Construction detail drawings	90
Weldment and assembly drawings	30
Shop fabrication	15
Work by technicians	10

It is estimated that the first loop will be assembled by the end of April, 1961.

b. Remote Capsule Assembly - The procedure and techniques for the remote assembly of the dry capsules have been developed. The drawings for the capsule modification and cask for handling the fuel specimens are almost completed. The assembly fixtures are being fabricated.

c. Development of Transparent Meltdown Facility - Design changes on the transparent slot liner meltdown facility, which were begun at the close of the last report period, were completed. Seven Zircaloy inner subassemblies of the new design were also fabricated, complete with Zircaloy and graphite liners for secondary protection of the steel from molten uranium.

V. NUCLEAR TECHNOLOGY AND GENERAL SUPPORT (040400)

A. Applied Nuclear and Reactor Physics

1. Experimental

a. Fast Neutron Capture Cross Section of Indium - The fast neutron capture cross section of In^{115} (n,γ) In^{116} (13 sec) was measured using an activation technique. The measured cross section is shown in Figure 15. The statistical error of each point due to counting is ±5% while the error in the absolute normalization is approximately ±20%. The normalization was obtained relative to the 54-minute indium activity which in turn was standardized against the known thermal neutron activation cross section for In^{116} (54 min) of 155 ± 10 bn.*

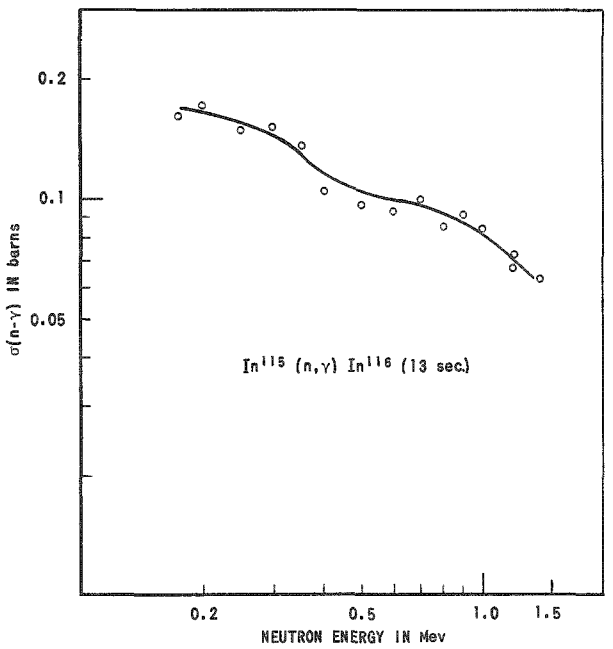

Figure 15

Fast Neutron Cross Section of Indium

b. Fission Cross Section Measurements - In conjunction with a precise measurement of the U^{235} fission cross section in the neutron energy range 10 kev to 300 kev, it was necessary to determine carefully the low energy neutron background existing near the accelerator's neutron producing target. Using B^{10} and Li^{6} detectors a careful mapping of the background intensity over the desired area was completed. In addition it was shown that this background is primarily due to very low energy neutrons.

---

* D. J. Hughes and J. A. Harvey, "Neutron Cross Sections," (1955).

c. Maintenance - 3-Mev Van de Graaff Accelerator - A large fraction of the month was consumed in carrying out major instrumental changes. A large pumping system was installed to permit rapid service of the accelerator. Downtimes of 12 to 15 hours are now cut to 1 to 3 hours with a corresponding increase in machine duty cycle.

The magnetic bunching system was installed and initial tests completed satisfactorily. This unit was proved capable of producing a 1 mμs proton burst having a peak pulsed intensity of > 1 ma and a duty cycle of up to 1%. These are, indeed, short and very intense bursts. Ultimately this unit will increase the efficiency of the fast neutron scattering measurements by up to a factor of ten. Simultaneously there will be a considerable improvement in the quality of the measured data. As a result of the initial magnet tests, relatively minor instrument adjustments are now being carried out.

d. Fabrication of Neutron Scintillation Detector - In the November, 1960, Progress Report (ANL-6269) mention was made of results reported at Chalk River on a slow neutron scintillator composed of a lithium fluoride-zinc sulphide mixture in lucite which offered improved neutron efficiency and discrimination against gamma radiation. An effort has been made to develop a convenient manufacturing method and also to evaluate the performance of such slow neutron scintillators. A very useful method has been found to make a system consisting of a corrugated scintillator mounted on a lucite light guide. The light guide is made first by heating and pressing lucite molding powder in a mold; then its corrugated surface is covered with the scintillator mixture of lithium fluoride, silver-activiated zinc sulphide and lucite, and heat and pressure is applied. The result is a scintillator directly molded onto the surface of its light guide. This represents an improvement over the device described by the Chalk River personnel in which the scintillator and light guide consisted of two pieces connected with high viscosity fluid. This procedure has been developed with natural lithium fluoride. Lithium fluoride enriched in the lithium-6 isotope has been obtained and tests with a detector built according to the above prescription are expected to show an efficiency for thermal neutrons of the order of 20%, based on tests performed to date with the natural lithium scintillator.

e. Technique for Checking Instrument Functions - A nitrogen-filled ion chamber has been operated with a variable direct voltage upon which was superimposed a 22 cycle/sec ripple. The chamber was placed in a neutron flux which produced a direct current of 12 microamperes upon voltage saturating of the detector. The alternating response of this instrument and its associated circuit was measured on an oscilloscope. As long as the applied d-c voltage on the chamber was insufficient to produce saturation, the alternating voltage component was effective in producing an alternating ion current of appreciable magnitude through the chamber. However, as the direct

voltage was increased to achieve saturation, the alternating component was observed to fall to a small value. The current limiting action of the ion chamber was due simply to its capacitive impedance without the effect of the ionization of the gas.

This behavior suggests that an alternating signal may be used to indicate malfunctioning of conventional power level circuits used on reactors. If the alternating component becomes higher than a preassigned level, it would provide an indication that the current chamber is being operated in an undersaturated state. If the alternating current should fall to zero, an open circuit would be suspected since even with voltage saturation there is a very small alternating current. The magnitude of the a-c signal also varies with the amount of ionization in the chamber. It is proportional to the flux, and so any warning circuitry must be based on the ratio of the a-c component to the d-c level.

Thus, through a relatively simple modification of the usual power level circuits a means would be available to check continually on the presence of high voltage applied to the detecting chamber, the degree of voltage saturation in the chamber, and the circuit continuity.

f. ZPR-VII High Conversion Critical Experiments - The start of these critical experiments is still delayed, pending receipt of Commission approval of the addendum to the ZPR-VII Hazards Report. In the meantime, preparations are continuing on some of the nonroutine aspects of the program of measurements planned. These include preparations for automatic measurement of control rod worth and determination of resonance escape probability by gamma-gamma coincidence counting of the Np^{239} formed by U^{238} capture.

The automatic control rod position indicator and the counting channels to be used in recording the associated change in flux level of the reactor have been operated in a core containing no fuel. It was found that spurious counts arise in the pulse counter channels when the control rod switch is operated. Steps have been taken to eliminate these unwanted counts. With the rod motor power supply located remotely from the linear amplifier, it was found that the spurious pulses were picked up through the pre-amplifiers. Accordingly, the pre-amplifiers were modified by improving the grounding of cable shields and bypassing the B+ and filament circuits to ground with ceramic capacitors, thus eliminating that source of pickup. However, the control rod power supply is normally mounted close to the linear amplifiers and so it has been relocated to eliminate noise which would be picked up directly in those amplifiers. The equipment is now ready for use in the Hi-C program.

Coincidences between three pairs of gamma rays associated with the decay of Np^{239} have been measured to determine the most favorable combination for the determination of U^{238} captures. With the window width

set at 1%, to minimize the background due to fission product gamma rays, the results of cadmium ratio measurements were as follows:

Coincidences	Cadmium Ratio
106 and 103 kev	2.49 ± 0.04
106 and 226 kev	2.55 ± 0.04
106 and 289 kev	2.57 ± 0.05

These values are to be compared with the cadmium ratio of 2.50 ± 0.03 observed for irradiated U^{238} foils from which the neptunium had been extracted chemically. The ratios are seen to be in good agreement. Because of intensity considerations, observation of the coincidences between the 106 and 103 kev radiations is preferable for the proposed measurements of resonance escape probability.

g. BORAX-V Superheater Critical Experiment - In the February Progress Report the results of calculations on the effect of flooding of a central and peripheral superheater zone were reported. Because of the magnitude of the reactivity effect associated with this potential hazard, the core design has been modified to provide water-tight caps for each superheater cluster as well as a water-tight container for each group of three clusters per quadrant for the more reactive central superheater zone geometry. This will reduce the possibility of flooding several clusters at once during operation with significant void volume in the superheat region. The calculated magnitude of other effects has indicated that extreme caution is required in the operation of the superheater system. The relatively small prompt temperature coefficient and the limited heat transfer from the voided superheater fuel to the moderator during any excursion serve to limit the effectiveness of inherent shutdown mechanisms in the event of an excursion. Preparations of a Hazards Summary Addendum covering the superheater criticals is nearing completion.

2. Theoretical

a. Resonance Parameter Systematics - In order to simplify analysis of fast neutron inelastic scattering and capture cross-section data, compilations of neutron strength functions formulated according to the optical model have been prepared in both tabular and graphical form. The objective of this program is the determination of average resonance parameter systematics with sufficient accuracy to obtain good estimates of cross sections and to deduce significant nuclear physics information from the measurements

b. Coupled Fast-Thermal Reactors - A simple program is being written for the IBM-704 in order to determine the change with time of the concentrations of various isotopes, particularly those present in the blanket

regions of a coupled system. The program is to be used in conjunction with the one-dimensional diffusion code RE-122. The procedure will be semi-automatic so that a series of burnup-buildup time steps can be taken during one session at the console of the computer.

c. CP-5 Converter Physics Analysis - The neutron fluxes available within an hypothetical converter tube assembly located in the graphite region of CP-5 have been calculated using the DSN code. For an assembly containing 600 gm of U^{235} the total fast flux is approximately 6×10^{11} n/(cm^2)(sec), while the thermal flux can be made as small as necessary by using boron in the innermost tube of the assembly. The fast flux can be increased by increasing the amount of U^{235} within the converter tube. However, the gain in flux will not be in direct proportion to the increase in uranium owing to the large thermal depression in the uranium. Doubling the amount of fuel will increase the fast flux by a factor of approximately 1.5. The reactivity effect of this facility will be small and burnup of U^{235} will be less than 0.3%/yr at a CP-5 operating power of 4 Mw.

d. Mathematical Methods - The code RE-129J now solves the one-dimensional reactor kinetics equation for a limited range input and limited thermal expansion followed by a shutdown described by the following equations:

$$\frac{dk}{dt} = \frac{12}{r_0}\int_{t_0}^{t} \frac{P}{M_2}\, dt = -12\frac{r}{r_0}$$

$$\frac{1}{M_2} = 3.3\left(1 - \frac{\int_0^{t_0} n\, dt}{\int_0^{t} n\, dt}\right)$$

$$P(t) = 3.2 \times 10^2 \left\{1 - \frac{3\, r(t+\Delta) - r(t)}{\sqrt{50 \cdot \frac{1}{3.3} M_2}}\right\}\int_{t_0}^{t} n\, dt$$

A series of problems have been run successfully.

There have been many difficulties encountered in the solution of the coupled reactor kinetics equations by the standard numerical methods used for differential equations. Because of these difficulties an attempt has been made to solve these equations by an extension of the collocation method for integral equations described in ANL-6132. The exceedingly cumbersome equations are in the process of simplification. Also under investigation is an adaptation of the single reactor equations considering the reactivity and an average neutron lifetime which are functions of the coupling parameters.

e. Multigroup Resonance Escape Probabilities - In the case of a mixture of absorbers, the following expression is commonly used to associate the resonance escape probability p, the absorption cross section Σ_a and the group transfer cross section Σ_R:

$$1 - p = 1 - \prod_i p_i = \frac{\Sigma_a}{\Sigma_a + \Sigma_R} = \frac{\sum_i \Sigma_{a_i}}{\sum_i \Sigma_{a_i} + \Sigma_R} \tag{1}$$

The index i ranges over all materials of the mixture.

The following approximations were examined:

$$1 - p_i = \frac{\Sigma_{a_i}}{\Sigma_{a_i} + \Sigma_R} \tag{2}$$

$$1 - p_i = \frac{\Sigma_{a_i}}{\Sigma_a + \Sigma_R} \tag{3}$$

and expressions derived for the error involved in their use depending upon whether one required $\sum \Sigma_{a_i} = \Sigma_a$ or $\prod_i p_i = p$.

Whereas Eq. (1) is consistent with the conditions:

$$\sum_i \Sigma_{a_i} = \Sigma_a \tag{4}$$

and

$$\prod_i p_i = p \tag{5}$$

the approximations (2) and (3) are not.

If one assumes that Eq. (5) holds, the average of the results obtained from Eqs. (2) and (3) for

$$\sum_i \frac{\Sigma_{a_i}}{\Sigma_a}$$

is found to be unity to terms of order $(1 - p_i)^3$.

If one assumes that Eq. (4) holds, the average of the results obtained from Eqs. (2) and (3) for

$$\prod_i \frac{p_i}{p}$$

differs from unity by an amount

$$\frac{p - 1}{2\,p^2} \sum_j \sum_{i>j} \frac{\Sigma_{a_j}\,\Sigma_{a_i}}{(\Sigma_a + \Sigma_R)^2}$$

plus higher order terms.

In either case, the use of the average of the results obtained from the approximations (4) and (5) reduces the error as compared with the use of either approximation by itself.

B. Reactor Fuels Development

1. Ceramic Fuels

a. Lanthana-Urania - Work on the lanthana-urania system was continued. Microstructures of air sintered compacts subjected to 1675° C and 1450° C heat treatments are presently under examination. Specimens containing more than 60 w/o urania subjected to the longer heat treatments possessed high porosity near the exposed surfaces. Weight losses of these specimens were appreciable in comparison to specimens having lower urania contents. Microstructural changes suggest that urania has volatilized preferentially along the grain boundaries.

X-ray diffraction examination indicated that uranium depletion has occurred on the pellet surfaces. Selected compositions were submitted for chemical analysis to determine metal concentrations and stoichiometry of heat treated specimens.

A modification of the vacuum-uranium chip anneal has been used in preparing samples for chemical analysis. A fused quartz hourglass bulb arrangement was made in which a sample is placed in one bulb and uranium chips as a getter material in the other. After a heat treatment at 900° C for 210 hours, the samples were isolated by sealing the capillary between the uranium bulbs. Specimens were submitted for chemical analysis to determine U^{+4} content.

b. Urania-Thoria - The investigation of the thermal expansion behavior of air sintered U_3O_8-ThO_2 solid solutions and hydrogen sintered UO_2-ThO_2 solid solutions was initiated (see February Progress Report). Compositions being studied are ThO_2, UO_2, and solid solutions in the range of 2.5 m/o UO_2 to 70 m/o UO_2.

Thermal expansion is being determined by the dilatometric method to a maximum temperature of 1600° C. The furnace is a tantalum resistance element operating in a vacuum. In operation the expansion of the sample displaces the core of a linear transformer and the output of the transformer is fed through an exciter-demodulator to a potentiometer recorder. The magnification of sample expansion is 348X with this apparatus. Measurements are being made of the equilibrium change in length at several temperatures up to the maximum of 1600° C.

c. Uranium-Thorium Sulfide - The thermal expansions of US and ThS were determined for the first time in a vacuum interferometer apparatus. The US sample was an older one, analyzing 91.6% US phase, whereas the ThS sample contained 97.5% ThS phase. The coefficients are given below along with values published for UO_2 and ThO_2 for purposes of comparison:

Table IX. Linear Coefficients of Thermal Expansion in in./in.-° C x 10^{-6}

US	UO_2	ThS	ThO_2
10.0 (0-100° C)	9.1 (27-400° C)	9.2 (0-100° C)	7.1 (20-300° C)
11.2 (100-500)	10.8 (400-800)	9.5 (0-500)	9.0 (20-700)
12.8 (500-930)	12.9 (800-1260)	10.2 (0-975)	10.4 (20-1500)

A series of US-ThS mixtures have been prepared and pelletized from homogenized powder. This series, which includes 100 m/o US, 75 m/o US-25 m/o ThS, 50 m/o US-50 m/o ThS, 25 m/o US-75 m/o ThS, and 100 m/o ThS, will be fired at 1800°, 1900° and 2000° C and run through a number of property determinations.

A 10:1 mixture of H_2O_2/H_2SO_4 has been found to be a much more satisfactory etchant for US polished sections than was the 6% H_2SO_4 in water. This mixture etches the grain boundaries and Widmanstätten pattern without staining the matrix material as did the H_2SO_4 solution. The action of this new etchant is progressive over a time period of 45 seconds.

The US Widmanstätten structure was studied at magnifications of up to 2000X and was found to consist of grooves of a stepped nature rather than a precipitated solid phase as previously surmised. The grooves fall on straight lines along crystal planes except where they terminate in

pores and become noticeably curved. This structure is not fully understood at the present time. Unetched ThS fired at 2000° and 2100° C shows very large grains averaging 150-160 microns containing a similar Widmanstätten pattern. In this case, however, high magnification shows that there is a solid phase of ThO_2 or ThOS precipitated along the crystal planes.

2. Properties of Metals and Alloys

a. Thermal Properties of U-Fs - The data on specific heat, heats of transformation and heat of fusion as determined by the University of Denver (under subcontract to the Laboratory) are essentially complete. The only exceptions are (1) heat of fusion on the three fissium alloys and (2) some additional data on the 3 w/o alloy. Data on uranium and on U-5 w/o Fs are given in Tables X and XI.

Table X. Heat Content of Uranium

Temperature (° C)	Heat Content (cal/gm)	Temperature (° C)	Heat Content (cal/gm)
0	0	750	30.7 ±0.3
200	5.3 ±0.1	800	37.7 ±0.5
300	8.7 ±0.2	900	42.3 ±0.5
400	12.6 ±0.2	1000	46.9 ±0.5
500	16.7 ±0.2	1100	51.5 ±0.5
600	21.0 ±0.2	1150	64.6 ±0.8
650	23.2 ±0.3	1200	66.4 ±1.2
700	28.4 ±0.3		

Heat of Transformation $\alpha = \beta$ @ 662° C, 3.3 ± 0.1 cal/gm.

Heat of Transformation $\beta = \gamma$ @ 772° C, 4.6 ± 0.1 cal/gm.

Heat of Fusion @ 1133° C, 11.0 ± 0.3 cal/gm.

Table XI. Heat Content of Uranium-5% Fissium Alloy

Temperature (° C)	$\alpha + \delta + U_2Ru$	$\alpha + \gamma + U_2Ru$	γ and $\gamma + U_2Ru$	Equilibrium (constructed)
0	0	0	0	0
200	5.3 ± 0.1	5.8 ± 0.1	5.8 ± 0.1	5.3 ± 0.1
300	8.3 ± 0.1	9.3 ± 0.2	9.3 ± 0.2	8.3 ± 0.1
400	11.4 ± 0.1	13.0 ± 0.2	13.0 ± 0.2	11.4 ± 0.1
500	15.6 ± 0.2	17.4 ± 0.2	17.4 ± 0.3	15.6 ± 0.2
550	18.0 ± 0.2	-	-	18.0 ± 0.2
600	-	22.0 ± 0.3	22.0 ± 0.3	23.1 ± 0.7
700	-	-	26.7 ± 0.4	29.8 ± 1.2
800	-	-	31.8 ± 0.4	38.6 ± 1.6
900	-	-	36.9 ± 0.5	43.7 ± 1.7
1000	-	-	42.0 ± 0.5	48.8 ± 1.7
1050	-	-	45.3 ± 0.8	51.1 ± 2.0

Heat of Transformation $\alpha + \delta + U_2Ru = \alpha + \gamma + U_2Ru$ @ 560° C, 2.8 ± 0.4 cal/gm.

Heat of Transformation $\alpha + \gamma + U_2Ru = \gamma + U_2Ru$ @ 630° C, 2.0 ± 0.4 cal/gm.

Heat of Transformation $\gamma + U_2Ru = \gamma$ @ about 740° C, 3.6 ± 0.4 cal/gm.

The heat of fusion reported is substantially lower than values reported in the literature. There appears to be some reason to doubt the validity of the literature values; however, this discrepancy is being checked carefully.

3. Corrosion Studies

a. Aluminum Powder Products for Fuel Element Cladding - Under subcontract to the Laboratory, Armour Research Foundation has succeeded in fabricating a few inches of powder product A288 tubing, using a bridge type die. Dimensions (including tolerances) were satisfactory, and corrosion resistance at 290°C and 360°C (after four and five weeks, respectively) is perhaps satisfactory In particular, there is no preferential corrosion at the junctions where the four metal streams meet to form the complete tube. Tubing produced from "as-atomized" and from 70 hour milled powder is in corrosion test; the amount of milling required to produce adequate creep properties is not yet known.

Productior of closures on powder product tubes presents a problem because conventional welding would destroy the powder product structure and therefore the strength of the bond. Atomics International has developed a eutectic bonding process using silver. Recently the process has been improved through the use of more precise temperature and pressure controls However, it still has not been possible to produce closures with consistently satisfactory corrosion resistance.

b. Lightweight Alloy for Liquid Mercury - The search for a corrosion resistant alloy compatible in high temperature mercury continues. Sheet samples of three metallurgical types of titanium alloys were tested. At 370°C and 100 psia (argon) under static isothermal condition, a beta-titanium alloy (Ti-13 w/o V-11 w/o Cr-3 w/o Al) suffered an unusual cracking attack in both the liquid and vapor phases of mercury. The propagation of these cracks showed both inter- and transgranular paths. Slight cracking was also observed in the alpha, and alpha plus beta, titanium alloys (Ti-5 w/o Al-2.5 w/o Sn and Ti-6 w/o V-4 w/o Al respectively). Such cracking was not observed on the rod form alpha-titanium alloy samples (Ti-5 w/o Al-2.5 w/o Sn) in previous tests. The difference in microstructure and hardness between the original and tested sheet specimens was not pronounced. It is not certain that a stress relief would improve this situation, however, plans have been made to investigate this possibility.

The beta-titanium alloy has shown a higher weight loss in liquid mercury than either alpha, or alpha plus beta, alloys during the same period of exposure. This test result provides the basis for further study on the alpha and alpha plus beta alloys

A thermal convection loop is being built to evaluate the mass transfer effect of the alloys in high temperature mercury.

4. Nondestructive Testing Methods

a. Ultrasonic Techniques - Studies of Lamb waves, mentioned in the Progress Report for November, 1960, (ANL-6269) have been continued. Attempts have been made to extend the Lamb wave attenuation studies in brass to larger D/T ratios by operating at 10 and 20 megacycles. It was not possible at higher frequencies to find a mode where the phase velocity of the mode equals the longitudinal velocity when the frequency is 10 or 20 megacycles. To find suitable modes, it was necessary to operate the crystal off its resonant frequency. However, the energy obtained when the crystal is pulsed at such frequencies is not sufficient to make Lamb wave attenuation measurements.

b. Neutron Techniques - Because neutrons have little influence on normal photographic emulsions, it is necessary for detection to use intermediate converter materials next to the film. These materials emit photographically detectable radiation when bombarded with neutrons, and thereby improve the photographic speed of the detection process.

One of the characteristics of the various neutron image detection methods which must be measured in order to evaluate them properly is the image sharpness, or resolution, which can be obtained. A method of measuring this is to prepare an image containing an abrupt density change, and to measure the change in film density versus distance across this edge. Recording microdensitometers are commonly used for this purpose. The commercially obtained recording densitometer presently available for use was designed primarily for other applications and in many ways it was found unsatisfactory for the problem. To solve the immediate problem of obtaining these sharpness data, a relatively simple photomultiplier tube scanning unit was designed and constructed. This unit employs a 931-A photomultiplier tube which is manually scanned across the projected image of the negative under study. A comparison of several characteristics of the designed unit and the commercial device are as follows:

	Developed Unit	Commercial Unit
Slit Width	0.4 mils	0.04 mils
Travel	0.001 in. steps	continuous
Upper Density Limit	at least 4.0	1.7
Magnification	20X	

Some sharpness data have been obtained using this developed unit and some preliminary data can now be reported. The transfer method using gold screens has yielded the best image sharpness of the metal screens tested. Some slight sharpness improvement was detected for the

thin screens (0.003 in. and 0.005 in.) over that obtained using the thicker screens (0.010 in.). The transfer method using indium screens yielded the second best sharpness result and again the thin screens (0.005 in. and 0.010 in.) showed a slight improvement over thicker ones (0.020 in. and 0.030 in.).

Of the direct exposure methods, rhodium showed the best sharpness, with no change detected over the thickness range from 0.003 in. to 0.010 in. Silver and indium screen direct exposures were next, in that order, with no sharpness change noted over a screen thickness range of 0.005 in to 0.030 in. It should also be noted that for both silver and indium direct exposures (and also for gold screen direct exposures) there is more definite evidence of increased image contrast on the film placed behind the screen (away from the neutron source) than in the film placed on the neutron side of the screen. Cadmium and gold direct exposures have yielded the poorest image sharpness. In the case of cadmium screens, the front film (toward the neutron source) has much better sharpness than the back film. This is particularly true for cadmium screen thicknesses greater than 0.005 in. The front film sharpness seems to be relatively independent of cadmium thickness over the range of 0.001 in. to 0.020 in. Gold screen direct exposures do not show a detectable change in image sharpness over the thickness range of 0.003 in. to 0.010 in. However, some sharpness improvement was noticed on the back film over the front film using the gold screens.

Further efforts aimed toward confirming these data and aimed at explaining some of the observed effects are currently in progress.

C. Reactor Materials Development

1. Irradiation Damage in Steels

a. Pressure Vessel Steel SA-212B - The gamma spectrum of two samples of irradiated SA-212B (MTR ANL-26 irradiation) was scanned with a 4 in. NaI crystal scintillation detector connected to a 100-channel analyzer for evidence of the thermal neutron transmutations of the isotopes of iron as described in the February Progress Report. The resolvable 1.10-Mev gamma for Fe^{59}, which lies approximately between the two cobalt-60 gammas, was not observed. A manganese-54 gamma line was found. The mechanism of formation is tentatively identified as an n-p reaction in the 1-Mev neutron energy region.

Samples of pure cobalt-free iron are being solicited for a continuation of the studies of the transmutation mechanism in the isotopes of iron since the end product is the transformation of Fe^{59} to Co^{59} which is then transformed to Co^{60}. A short-time irradiation in the CP-5 is contemplated.

b. Magnetic Properties - Approximately a dozen irradiated SA-212B specimens with known impact and hardness properties (remnants of multi-notch impact bars from the ANL-26 irradiation) were prepared into 0.204 in. diameter by 0.950 in. long magnet bars. Unirradiated, soft and hardened SA-212B magnet bar standards were magnetically examined in the semi-finished condition for uniformity of heat treatment and preparation. The magnet bar standards showed the expected variations in permeability associated with their hardness levels; the hardest bars (R_C 45/46) had the lowest permeability.

D. Reactor Components Development

1. Development of Manipulators for Handling Radioactive Materials

Cables used for the control of servo master-slave manipulators and slave robots must have many individual conductors, be durable, and extremely flexible. High flexibility is required so that the cable can be routed easily and with a minimum of friction. Since such cables are not commercially available, an experimental cable was fabricated and fatigue-tested.

The individual conductors in this cable are insulated with 0.012 in. of polyvinyl chloride and are composed of 105 strands of AW6 40 bare copper wire. Twelve of these conductors were twisted and tied together with flat fabric cords to make a bundle. Seven such bundles were twisted together - the entire construction being very much like that of a standard rope. This assembled cable of 84 conductors was lubricated with talcum and then covered with a neoprene tube having a one inch inner diameter and a $\frac{1}{8}$ in. thick wall.

The cable was fatigue tested by pulling it around three 6 in. diameter pulleys arranged so that the cable was subjected to one 180° reversing bend each cycle. Tension on the cable was 60 pounds. After 150,000 cycles, one conductor broke. The test was continued until two more conductors broke at 300,000 cycles. It is planned to test this type of cable further with the hope of gaining better fatigue characteristics through the use of other lubricants.

E. Heat Engineering

1. Dynamic Characteristics Using Correlation Techniques

Computing code RE-245, which computes the autocorrelation function and the power spectrum of the steam void fraction on the basis of gamma-ray measurements, has been completed. The program was tried on one set of data and it was noticed that in its present form it gives results with a large scatter unless a very large amount of input data (long records) are used. Methods of modification are being investigated for obtaining reasonably stable results with shorter records. For the program three records are needed, one obtained during the actual run beaming the gamma-rays through the desired point of the boiling channel, the others beaming the rays through hot full, and empty channels.

2. Hydrodynamic Instability Studies

A series of tests are currently being run on a $\frac{3}{8}$-in. diameter test section with a $\frac{1}{2}$-in. diameter riser. These tests fit into an overall program measuring the effect of geometry, pressure, water level, and inlet temperature on the power input, amplitude, and frequency during oscillations. The automatic power control system has been installed and is ready for operation.

The heating power to a rectangular test section in the small scale loop is being oscillated sinusoidally, and the void response is measured. A series of transfer function measurements have been taken at 41 atm for various powers, flow rates, and subcooling temperatures. The taking of data at 41 atm has been completed, and additional measurements at a few higher and lower pressures are now being carried out.

3. High Void Natural Recirculation Studies

This experiment is designed to study natural recirculation up to 50% voids in a 12-in. riser. The equipment was formerly referred to as the SLURREX mockup. Preliminary tests revealed that the air-water separation unit design results in high downcomer void carryunder. Also insufficient distance was allowed between the fluid surface and the air exit point.

At the high voids, the splashing violence of the fluid surface due to the bubbling air choked off the air exit line. This caused water to become trapped in the exit line and occasionally to flow out the top. A new separation unit has been designed and is being fabricated.

4. Boiling Liquid Metal Experiments

a. Sodium Loop - The small scale loop design for studies of boiling liquid metals is essentially complete. Materials and instrumentation are being ordered and fabrication of loop components is scheduled to begin in early April. Initial tests will be with sodium and will be aimed at measuring vapor volume fractions and two-phase frictional behavior in a flowing system.

A small, low temperature NaK-argon loop is being constructed to test the feasibility of measuring void fractions with an electromagnetic flowmeter.

b. Sodium Boiler - A design study of a natural circulation sodium boiler was initiated. The boiler is to provide saturated sodium vapor at pressures up to 3 atm for a variety of experiments. The primary objective of the design study is to develop a boiler with the capability of operating continuously for periods of up to one year. The main circulating portions of the boiler have been sized.

5. Heat Transfer from a Liquid-Liquid Interface

The purpose of the experiment is to investigate direct heat exchange between two immiscible liquids in the absence of a separating wall. It is hoped that the experiments will provide fundamental information about the process of nucleation in boiling as well as data on direct contact heat exchange between two liquids.

A very simple experimental apparatus has been designed. The test section is a rectangular container (6.35 cm by 7.61 cm by 12.5 cm), two sides of which are made of glass to permit the taking of motion pictures. An electrical resistance heater is used to supply energy to the bottom of the test section. The heat is transferred to the mercury, which partly fills the test section, and then through the mercury to a lighter liquid on top of it.

The experimental apparatus has been completed and some preliminary runs were made. However, experimental difficulties were encountered in the tests. It was known that mercury wets poorly practically all solid materials, but the extent of such non-wetting was quite unexpected. Because of the poor contact at the solid surfaces water could run down (about 1.5 cm)

along the solid wall to the heated plate and boil off this surface, instead of the mercury-water interface. In an effort to eliminate this difficulty, the bottom plate has been redesigned.

6. Packed Bed Studies

The problem of shutdown cooling for a packed bed irradiation experiment was examined in some detail. The problem is apparent for an accidental loss of coolant, and because of the required limited duration of coolant flow it is desirable to rely on cooling by radiation and conduction as soon as possible after normal shutdown. In this connection a survey of the literature revealed experimental high temperature thermal conductivity data for beds of UO_2 powders (in the size range of interest) in helium, argon, nitrogen, helium/argon and xenon/krypton mixtures. It was found that most of the data could be reasonably well correlated by the expression

$$\frac{k_{eff}}{k_g} = 1.8\left(\frac{k_p}{k_g}\right)^{0.43}$$

where

k_{eff} = bed conductivity

k_g = gas conductivity

k_p = particle conductivity.

This relation was used to predict the conductivity of a UO_2-ThO_2 bed in stagnant steam over a range of temperatures.

It is anticipated that a mechanical disconnect joint may be used on the high temperature steam side of the experiment. It was determined that couplings of the type being considered have been assembled and thermal cycled at temperatures to 650°C by ORNL. The leak rates encountered with helium were extremely small (on the order of 10^{-10} cm^3/sec at 25 atm pressure) indicating usefulness for the present application.

All components are completed for a second power feasibility study of induction heating for heat transfer to packed beds. The coil and transmission line is fabricated, high-purity iron particles have been obtained, and a fast response thermocouple is being fabricated.

F. Separations Processes

1. Fluidization and Fluoride Volatility Separations Processes

a. Direct Fluorination of Uranium Dioxide Fuel - Pilot plant fluorination of a six-inch bed of hydrogen-fired uranium dioxide pellets was carried out in a three-inch diameter column. Operating conditions

during the run were uranium hexafluoride production rate, 560 g/hr; fluorine utilization, 55 per cent; inlet fluorine concentration, 42 per cent (in nitrogen). This is the highest rate and efficiency obtained so far for hydrogen-fired pellets; however, the rate was limited by relatively poor heat transfer due to partial caking. Center of bed temperature control was maintained within 10 degrees of 530°C by regulation of the amount of inlet fluorine.

Tests were made in a glass mockup system of the new off-gas filter system. Separate sintered nickel bayonet filters were mounted in close-fitting chambers connected to the column with a one-inch pipe. No accumulation of fines was observed in a prolonged testing (~8 hr) of the automatic blowback system. The separate arrangement would facilitate filter replacement in a radioactive process application.

b. Processing Stainless Steel-Clad Fuel Elements - A two-zone fluid-bed reactor is being used to study chlorination and fluorination reactions for the decladding and dissolution of stainless steel-clad uranium dioxide fuel elements. The stainless steel cladding is reacted with chlorine in the lower zone. The chlorination products formed in the lower zone pass into the upper zone where they are converted to the tetrafluoride by reaction of hydrogen fluoride. Complete reaction of 35-mil type 304 stainless steel, closed end, tube specimens was demonstrated in less than four hours using 87 and 43 mole per cent chlorine in nitrogen at 625°C. Stainless steel (304, 35-mil) specimens ignited in 87 mole per cent chlorine gas at 645°C and caused sintering of the nonvolatile chloride and bed material.

Previous runs had shown an adherent nonvolatile chloride scale inhibited chlorination. Two runs were made at 580°C in which chlorine and steam were cycled in an effort to convert the adherent nonvolatile stainless steel chlorides to a powdery oxide, thereby increasing the effective chlorination rate. However, penetration rates of only 3.8 and 2.5 mils/hr were obtained in five- and four-hour tests.

Analysis of the off-gas scrub solution from previous uranium dioxide chlorinations showed a negligible total uranium loss of 0.007 per cent of the uranium dioxide charged.

c. Steam Hydrolysis of UF_6 to UO_2F_2 - Short-duration runs are being made to study the formation of fines encountered in the steam hydrolysis of uranium hexafluoride in a fluid bed. Normal growth rates were observed with starting beds of 200μ and coarser; finer beds showed fines formation shortly after the hexafluoride was introduced or after a period of little particle size change.

d. Plutonium Fluoride Studies - Plutonium hexafluoride reacts with bromine between 30° and 180°C to produce plutonium tetrafluoride and bromine pentafluoride as the major products. Bromine trifluoride is also formed as a side reactant. It has been demonstrated that the reaction involving the reduction of plutonium can be utilized to separate uranium hexafluoride from plutonium hexafluoride.

The gamma radiation decomposition of plutonium hexafluoride is being investigated. Irradiation of gaseous plutonium hexafluoride indicates that the decomposition ranges from approximately three per cent for a dose of 2.3×10^6 rad to about 13 per cent at 1.3×10^8 rad.

Work on the kinetics and mechanism of plutonium hexafluoride decomposition has been completed. The rate constants obtained at 140°, 161° and 173°C have been used to obtain the experimental activation energies of 15.9 ± 1.5 and 19.6 ± 0.7 kcal/mole for k_0 and k_1, respectively, which apply to the rate equation $-dp/dt = k_0 + k_1 p$. The rate equation is descriptive of a concurrent heterogeneous and homogeneous mechanism for the reaction $PuF_6\,(g) \rightarrow PuF_4\,(s) + F_2\,(g)$.

2. Chemical-Metallurgical Process Studies

a. Liquid Metal Solvent Studies - The solubility of lutetium and chromium in liquid cadmium may be represented by the empirical equations

lutetium (324°-557°C): $\log (\text{atom per cent}) = 7.328 - 7630\,T^{-1} + 1.745 \times 10^6\,T^{-2}$

chromium (450°-650°C): $\log (\text{atom per cent}) = 0.3994 - 2605\,T^{-1}$.

The partial molal heat of solution $\Delta\bar{H}$ and excess entropy of solution $\Delta\bar{S}_{xs}$ of chromium, manganese and cobalt in liquid cadmium have been computed from the temperature variation of the solubilities of these metals in cadmium. The values of these partial molal quantities at infinite dilution are as follows:

Solute	ΔH_∞ (kcal/mole)	$\Delta S_{xs\infty}$ (cal/deg mole)
Chromium	8.04	-9.40
Manganese	4.19	-1.09
Cobalt	22.9	3.06

Phase studies of the uranium-zinc system confirm the existence of a eutectic between the delta uranium-zinc intermetallic phase (U_2Zn_{17}) and uranium. A mixture of zinc and uranium (35 weight per cent uranium) was heated to 970°C under three atmospheres pressure in a tantalum crucible. The ingot that formed on cooling contained extensive regions of

eutectic structure. The two phases in the eutectic structure were identified as alpha uranium and the delta uranium-zinc phase. No intermediate phases between the delta composition and pure uranium were observed

The transformation of the epsilon uranium-zinc intermetallic phase ($UZn_{11.5}$) to the delta phase has been observed to occur at 880°C but not at 830° or 780°C. These observations are in agreement with thermal analysis data which place the peritectic temperature at 844°C On the basis of current information, it is not clear whether the delta and epsilon phases exist as two distinct phases at all temperatures, or if the delta phase exists as the high-temperature modification of the epsilon phase. Studies directed toward the clarification of the relationship between the two phases are being made.

Values of the coprecipitation coefficient for thorium and praseodymium when carried by the intermetallic compound $CeCd_{11}$ from liquid cadmium are 1.08 and 0.631, respectively. The coprecipitation coefficient of cerium when carried by the intermetallic compound $GdCd_6$ from liquid cadmium was found to be 0.34.

The vapor pressure of cadmium-uranium alloys has been measured as a function of composition using the continuous recording effusion apparatus. The vapor pressure-composition patterns indicated the existence of a single intermetallic compound corresponding to the empirical formula UCd_{11} and were in complete agreement with the results previously obtained by conventional methods for phase studies. This experimental procedure is now ready for use in investigating other less well-known systems.

Preliminary measurements of the magnetic susceptibility of the uranium-cadmium intermetallic phase, UCd_{11}, from room temperature to the boiling point of helium indicate that the susceptibility follows a Curie-Weiss relationship $[\chi = C/(T-\Delta)]$ with $\Delta = -29°K$ and $C = 1.21_9$. The effective Bohr magneton number for the uranium is 3.12. This value is reasonably close to 2.85, the value expected for spin only coupling in a system of two unpaired electrons. Whether these two electrons occupy 5f or 6d orbitals has not been determined.

The influence of magnesium on the distribution coefficient of uranium between the two partially immiscible liquid metals zinc and lead has been measured. At 601°C, the following preliminary values of the distribution coefficient (weight per cent uranium in zinc-rich phase/weight per cent uranium in lead-rich phase) were obtained: 1077, 286, 250, and 217 with magnesium concentrations (in weight per cent) in the lead phase of 0, 0.14, 0.27, and 0.75, respectively. The distribution of the magnesium favored the zinc phase over the lead phase in roughly a two to one proportion.

Attempts are being made to improve the preliminary value for the standard heat of formation, ΔH_f°, of $UF_6(g)$ by obtaining additional information concerning the composition of the residual products formed during the combustion. Preliminary experiments have demonstrated that about 98 per cent of the uranium that reacted formed uranium hexafluoride. The other two per cent of uranium mostly formed UF_3 and UF_4, with very small amounts of U_4F_{17}, U_2F_9, and UF_5 also being formed.

Improved boron nitride combustions in fluorine were achieved by using sapphire discs for sample supports. A disc of optically polished single-crystal aluminum oxide (Linde Co. sapphire) was found to be completely inert to fluorination in the experiments with boron nitride.

Satisfactory techniques have been developed for combustions of tantalum and niobium.

G. Advanced Reactor Development

1. High Power Density Fuel Element Design Studies

Experiments were performed on a high power density flat plate fuel box (Progress Report, January, 1961, ANL-6307, p. 61). The plates began to deform near the predicted divergence velocity. Non-linear hydrodynamic forces, coupled with the smallness of the plate spacing compared with the elastic properties of the plates, kept the plates from receiving a permanent set. At higher velocities the plates began to array themselves in groups of three rather than two and at the limit of the test, 10.5 m/sec maximum box flow rate, in groups of four.

2. Compact High Power Density Fast Reactors

The purpose of this work is to develop an efficient, compact fast reactor system using sodium vapor as the working fluid in a direct cycle system.

As part of the program a turbine unit using a simple uncooled wheel has been designed to investigate blade materials, bearings, and shaft seals. A combination axial and labyrinth seal using sodium liquid as a lubricant on the axial side with argon buffer between the air side is proposed. Standard ball bearings lubricated with an oil mist are to be used. Tentatively, titanium carbide has been selected for the seal stator and tungsten carbide for the seal runner.

The second phase of the turbine test program would use a turbine wheel with hollow blades cooled by flow from a feed line in the shaft. Temperature drop across the blades will be measured by thermocouples that terminate on a series of slip rings on the turbine shaft.

3. Fast Reactor Test Facility

As part of an advanced fast reactor program, a survey is underway to determine the need and potential value of an experimental facility for the evaluation of key parameters of new concepts. Preliminary studies indicate that such a facility should be versatile enough to cover the following design conditions:

a. 50 Mwt total power.

b. Power densities ranging from 0.1 to 1 Mw/liter.

c. Core composition including uranium alloys, oxides, cermets, and plutonium-fissium.

d. Maximum operating temperatures that are at least comparable to the highest steam conditions used in the most modern power stations.

Although the experimental facility would be designed initially for sodium as reactor coolant, the heat rejection system and control room would be common to possible future reactor systems utilizing other coolants.

4. Direct Conversion Studies

a. Cesium Plasma Cell - In several recent Monthly Progress Reports work on a cesium cell for direct conversion experiments has been discussed. This cell is shown schematically in Figure 16. Cesium vapor is supplied to the cell from special containers and the vapor pressure in the cell is determined by its temperature. The temperature of the cell and vapor is regulated by circulating heated silicone oil. The emitter is made from UC(40%)-ZrC(60%). It is separated from the collector by a distance of 0.6 mm. The collector has an area of 0.3165 cm^2 and is surrounded by a guard ring.

For a relatively constant value of cesium pressure and a particular emitter temperature (determined by optical pyrometry), the voltage-current characteristic of the cell is determined. Data must be taken with a fast-response recorder within a period of a few seconds during which the emitter temperature and electron emission can be held approximately constant

In Figure 17 three sets of results are shown. The insert at the right of each current-voltage trace shows the voltage-power relationship. The power maximum and maximum power density is shown for each set of parameters.

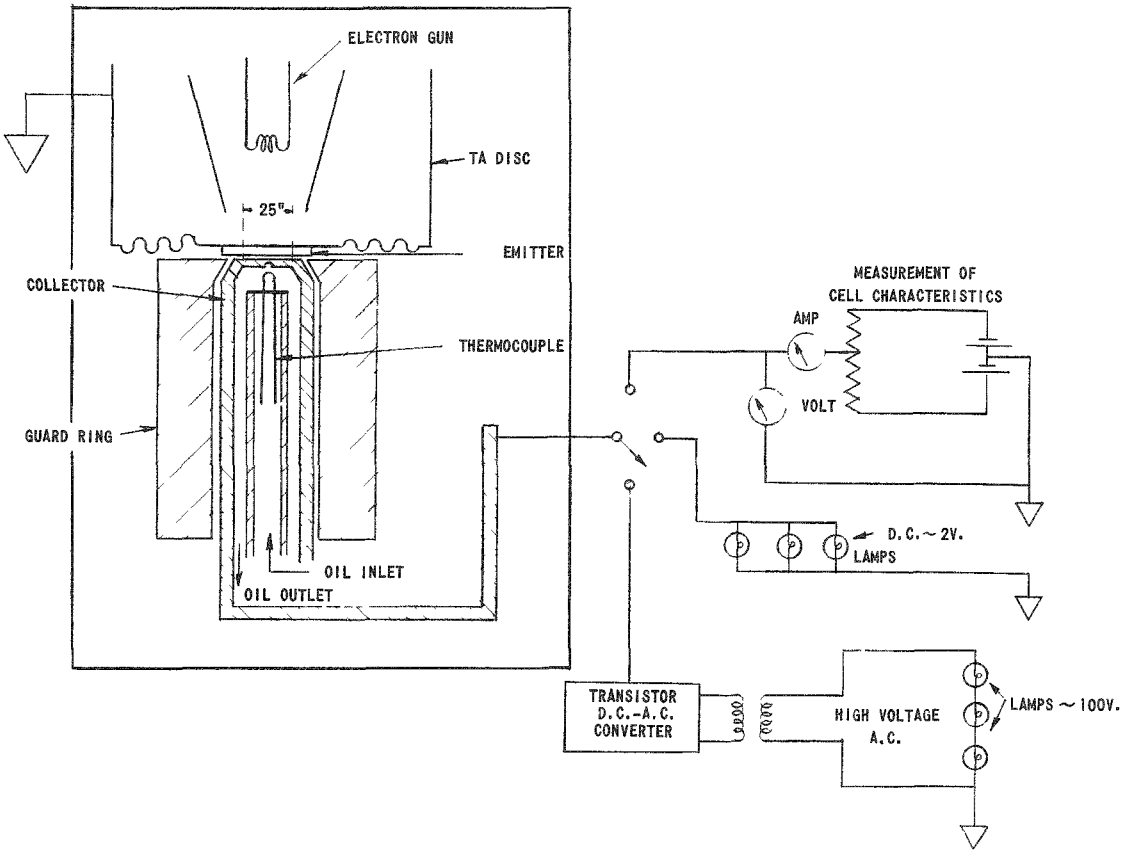

Figure 16

Plasma Cell with Test Instrumentation,
Lamp Loads, and D. C. -A. C. Converter

The electron current is counted as positive in the direction from the emitter to collector. The voltage is marked positive if the collector is more positive than the emitter. It is seen that the voltage and current have the same direction at positive voltages. At negative voltages the electron current flows against the retarding potential and can deliver power into a load. Only this portion is therefore usable for energy conversion.

Figure 17A shows the cell characteristics at a relatively low emitter temperature. At +4 volts the current increases rapidly, probably due to the first ionization potential level of cesium, which is at 3.8 volts. The current remains nearly constant from +4 volts down to -1.5 volts, then drops rapidly to zero, and at about -3.5 volts it goes to a negative value. At a negative value the cesium ion current exceeds the electron current.

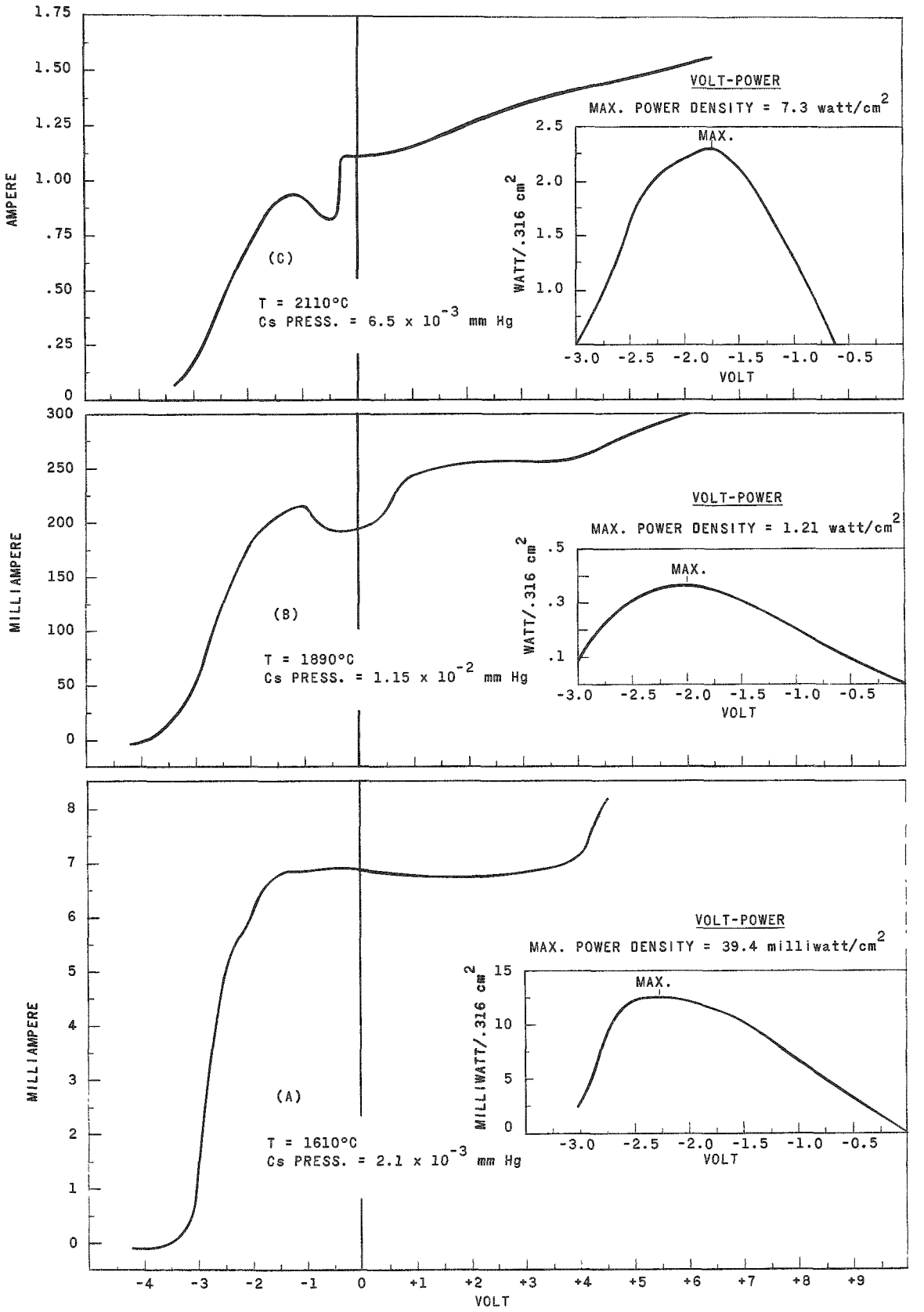

Figure 17

Cs-Plasma Cell Voltage - Current and Voltage Power Characteristics

Curves 17B and 17C are for higher emitter temperatures. The increase in current output follows the Richardson equation. At negative voltages the current has no flat portion, but decreases constantly. Also the power maxima are shifted to lower values. This indicates losses due to electron scattering and absorption, and lower energy losses within the plasma. The hump shows that a region of negative resistance exists and may produce oscillations.

Table XII presents measured values for emitter temperature, cesium pressure, short circuit current density (i.e. emitter and collector at the same potential), power density maximum, and the voltage at maximum power.

Table XII. Measured Characteristics of the Cesium Vapor Cell

T, °C	Cesium Pressure, mm Hg	Current Density, ma/cm^2	Maximum Power Density, $watts/cm^2$	Voltage at Power Maximum
1490	5.2×10^{-3}	1.18	0.001	2.5
1560	$6\,5 \times 10^{-3}$	5.00	0.011	2.5
1630	6.5×10^{-3}	18.2	0 035	2.5
1690	8.0×10^{-3}	36.3	0.078	2.25
1810	9.0×10^{-3}	183.5	0.335	2.25
1890	$1\,15 \times 10^{-2}$	664.0	1.21	2.00
1960	1.8×10^{-2}	950.0	1.81	2 00
2110	2.0×10^{-2}	4100	7.18	1.75
1610	2.1×10^{-3}	21 8	0.039	2.25
1650	4.5×10^{-3}	117.0	0 260	2.50
1845	8.2×10^{-3}	435.0	0.515	2.25
1900	2.0×10^{-2}	824.0	1.59	2.25
2005	1.2×10^{-2}	2530	5.06	2.00
2085	1.2×10^{-2}	8200	10.18	1.75

The output current densities of the cesium cell at high emitter temperatures reach many amperes while the voltages obtainable at power maxima are less than 2 volts. At high currents transmission losses can become prohibitively high. The transistorized D.C.-A.C. converter indicated in Figure 16 is used to convert the cell output to a high voltage and low current.

Figure 18 shows the circuit of the converter. No moving parts are involved. The output for several hundred volts consists of square waves of 600-700 cps. A conversion efficiency of 60 to 70% has been obtained; however, with new semiconductor constructions an improvement up to 90%

is expected. As shown in Figure 16 lamp loads with low voltage ratings were used in direct connection with the collector and high voltage lamps in connection with the converter.

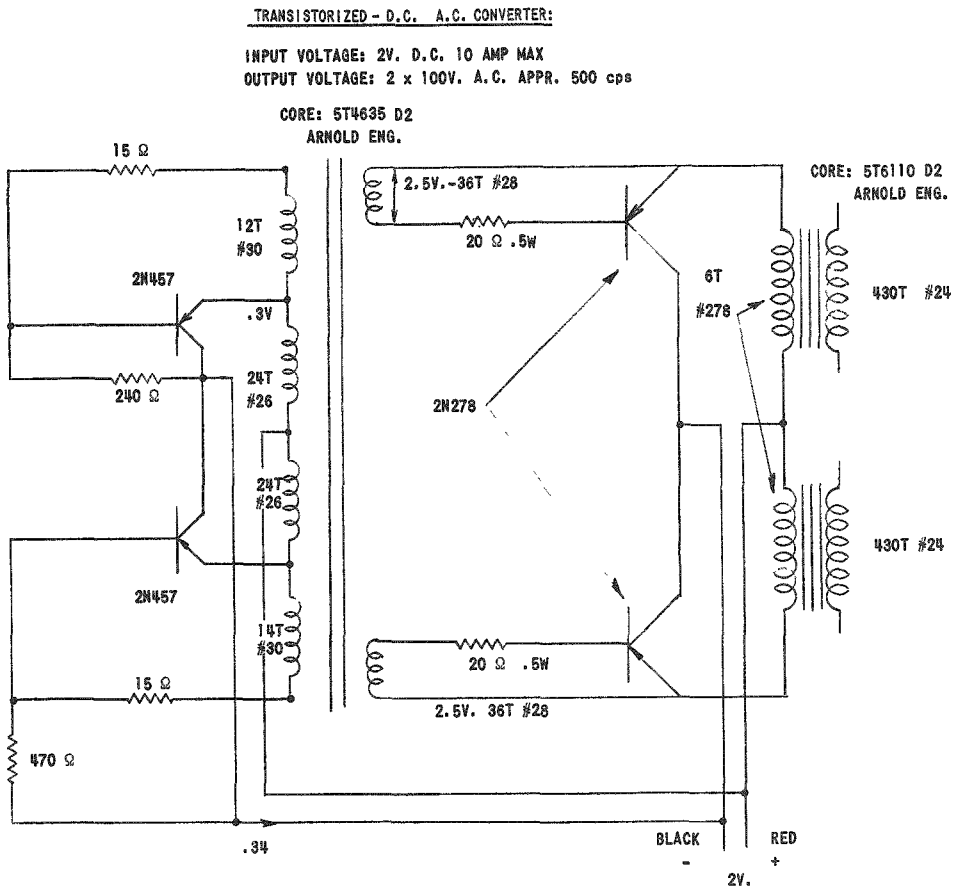

Figure 18

D. C. -A. C. Transistorized Converter

In a potential reactor design nuclear fission would supply the heat for the emitter. Fuel rods of high conductivity are necessary. While uranium monocarbide has a conductivity approaching that of a metal, the material is very brittle. Possible designs involve sheathing of the UC with tantalum and depositing the electron emitting material on the tantalum surface. Insulation and structural considerations, as well as radiation heat transfer capabilities, are limiting factors in the design.

VI. PUBLICATIONS

Papers

RADIATION LEVELS IN EBWR
Vincent C. Hall, Jr., and Robert H. Leyse
Nucleonics, 19, No. 3, 80 (1961).

N^{16} CONCENTRATION IN EBWR
Robert L. Mittl and Michel H. Theys
Nucleonics, 19, No. 3, 81 (1961).

THERMAL NEUTRON ABSORPTION CROSS SECTIONS BY THE PULSED SOURCE METHOD
J. W. Meadows and J. F. Whalen
Nuclear Sci. & Eng 9, 132 (1961).

RADIATION DAMAGE IN STEEL. CONSIDERATIONS INVOLVING THE EFFECT OF NEUTRON SPECTRA
A. D. Rossin,
Nuclear Sci. & Eng. 9, 137 (1961).

AGE OF FISSION ENERGY NEUTRONS TO INDIUM RESONANCE IN WATER
R. C. Doerner, R. J. Armani, W. E. Zagotta, and F. H. Martens
Nuclear Sci. & Eng. 9, 221 (1961).

ON THE MAXIMIZATION OF THE SENSITIVITY OF A FUEL ASSAY REACTOR
Henry A. Sandmeier
Nuclear Sci & Eng. 9, 260 (1961).

FAILURE OF NEUTRON TRANSPORT APPROXIMATIONS IN SMALL CELLS IN CYLINDRICAL GEOMETRY
J. A. Thie
Nuclear Sci & Eng. 9, 286 (1961).

CERTIFICATION OF ALGORITHM 13, COMPLEX EXPONENTIAL INTEGRAL
P. J. Radar and H. C. Thacher, Jr.
Communications of the Association for Computing Machinery, 4, No. 2, 105 (1961).

IRRADIATION GROWTH OF ZIRCONIUM-PLUTONIUM ALLOYS
J. A. Horak and H. V. Rhude
J. Nucl. Materials 3 (1) III (1961).

Papers

NONDESTRUCTIVE TESTING
Warren J. McGonnagle
McGraw-Hill Book Co. Inc., New York, New York (1961).

APPLIED GAMMA RAY SPECTROMETRY
C. E. Crouthamel, Ed.
London: Pergamon Press, 1960.

FREE ENERGIES OF FORMATION OF GASEOUS URANIUM, MOLYBDENUM, AND TUNGSTEN TRIOXIDE
R. J. Ackermann, R. J. Thorn, C. Alexander, and M. Tetenbaum
J. Phys. Chem. 64, 350 (1960).

STUDIES OF METAL-WATER REACTIONS AT HIGH TEMPERATURE: THE CONDENSER DISCHARGE METHOD APPLIED TO ZIRCONIUM-WATER REACTION
L. Baker, R. L. Warchal, R. C. Vogel, and M. Kilpatrick
Trans. Am. Nuclear Soc. 3 (1), 239 (1960) Abstract.

MONITORING A FUEL RUPTURE IN A NaK OR Na-COOLED OPERATING REACTOR
C. E. Crouthamel
Trans. Am. Nuclear Soc. 3 (1), 289 (1960) Abstract.

DECAY CHARACTERISTICS OF POTASSIUM-42 AND TELLURIUM-132
C. Gatrousis and C. E. Crouthamel
J. Inorg. and Nuclear Chem. 13 (1/2), 13 (1960).

THE FLUID-BED CONVERSION OF URANIUM HEXAFLUORIDE TO URANIUM DIOXIDE
I. E. Knudsen, N. M. Levitz, and S. Lawroski
Trans. Am. Nuclear Soc. 3 (1), 42 (1960) Abstract.

THERMAL NEUTRON CROSS SECTION OF REACTION $Cs^{137}(n,\gamma)Cs^{138}$
D. C. Stupegia
J. Nuclear Energy: Reactor Science, Part A 12, 16 (1960).

Papers

DOSE DISTRIBUTION IN THE ARGONNE HIGH LEVEL GAMMA IRRADIATION FACILITY
H. G. Swope
The Radiation Microbiology Conference, Quartermaster Food and Container Institute for the Armed Forces, Quartermaster Research and Engineering Command, Quartermaster Corps, U.S. Army, Chicago, Illinois
QMF and CI Report Nr. 26-60, 1960.

ANL Reports

ANL-5639 EFFECTS OF IRRADIATION ON THE EBWR FUEL ALLOY URANIUM - 5 w/o ZIRCONIUM-1.5 w/o NIOBIUM
J. H. Kittel

ANL-6117 THE FLUORINATION OF URANIUM FROM DRIED SOLIDS AND ITS APPLICATION TO THE FLUORIDE VOLATILITY PROCESS
C. E. Johnson and J. Fischer

ANL-6159 SPRAY FLUORINATION OF FUSED SALT AS A URANIUM RECOVERY PROCESS
J. D. Gabor, W. J. Mecham, A. A. Jonke, and W. A. Rodger

ANL-6160 EXAMINATION OF AN IRRADIATED PROTOTYPE FUEL ELEMENT FOR THE ELK RIVER REACTOR
L. A. Neimark

ANL-6171 KINETICS OF PARTICLE GROWTH IN A FLUIDIZED CALCINER
B. S. Lee

ANL-6255 GAS-COOLED REACTORS IN THE USA: A SURVEY AND RECOMMENDATION
R. H. Armstrong

ANL-6266 INSTABILITY STUDIES WITH EBR-I, MARK III
R. R. Smith, J. F. Boland, F. D. McGinnis, M. Novick and F. W. Thalgott

ANL-6293 AN ANALOGUE SOLUTION OF A REACTOR PERTURBATION INITIATED BY A METALLURGICAL PHASE TRANSFORMATION OF THE FUEL
Lawrence T. Bryant, Joseph C. Carter, and Marion J. Janicke

ANL Reports

ANL-6299 EBR-II DRY CRITICAL EXPERIMENTS. EXPERIMENTAL PROGRAM, EXPERIMENTAL PROCEDURES, AND SAFETY CONSIDERATIONS
L. J. Koch, W. B. Loewenstein, A. Lovoff, H. H. Hooker, H. O. Monson, R. L. Ramp and E. Hutter

ANL-6304 AN EMPIRICAL MODIFICATION OF NUCLEATION THEORY AND ITS APPLICATION TO BOILING HEAT TRANSFER
Yan Po Chang (University of Notre Dame)

ANL-6305 EBWR CORE IA PHYSICS ANALYSIS
R. Avery, K. Almenas, C. Carson, H. Iskenderian, and C. Kelber